Medical Robots, Constrained Robot Motion Control, and "Virtual Fixtures"

Russell H. Taylor

601.455/655

Disclosures & Acknowledgments

- **<u>This is the work of many people</u>**
- Some of the work reported in this presentation was supported by fellowship grants from Intuitive Surgical and Philips Research North America to Johns Hopkins graduate students and by equipment loans from Intuitive Surgical, Think Surgical, Philips, Kuka, and Carl Zeiss Meditec.
- Some of the work reported in this talk incorporates intellectual property that is owned by Johns Hopkins University and that has been or may be licensed to outside entities, including including Intuitive Surgical, Varian Medical Systems, Philips Nuclear Medicine, Galen Robotics and other corporate entities. Prof. Taylor has received or may receive some portion of the license fees. Also, Dr. Taylor is a paid consultant to and owns equity in Galen Robotics, Inc. These arrangements have been reviewed and approved by JHU in accordance with its conflict of interest policy.
- Much of this work has been funded by Government research grants, including NSF grants EEC9731478 and IIS0099770 and NIH grants R01-EB016703, R01-EB007969, R01-CA127144, R42-RR019159, and R21-EB0045457; by Industry Research Contracts, including from Think Surgical; by gifts to Johns Hopkins University from John C. Malone, Richard Swirnow and Paul Maritz; and by Johns Hopkins University internal funds.

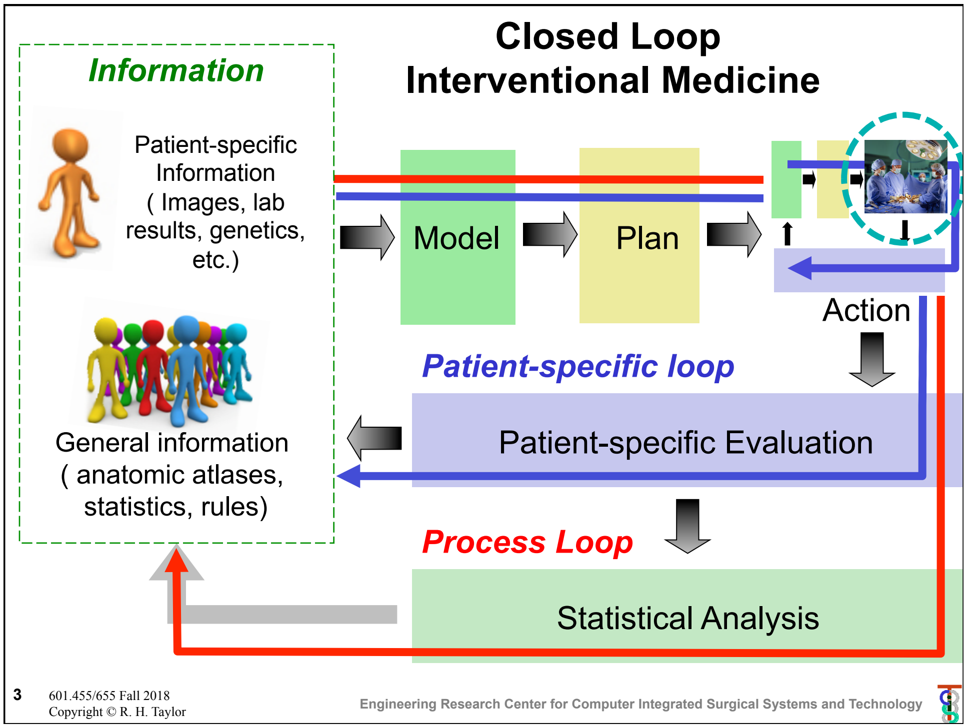
Closed Loop
Interventional Medicine
Information
Patient-specific Information (Images, lab results, genetics, etc.)
General information (anatomic atlases, statistics, rules)
Model
Plan
Action
Patient-specific loop
Patient-specific Evaluation
Process Loop
Statistical Analysis
3
601.455/655 Fall 2018
Copyright © R. H. Taylor
Engineering Research Center for Computer Integrated Surgical Systems and Technology

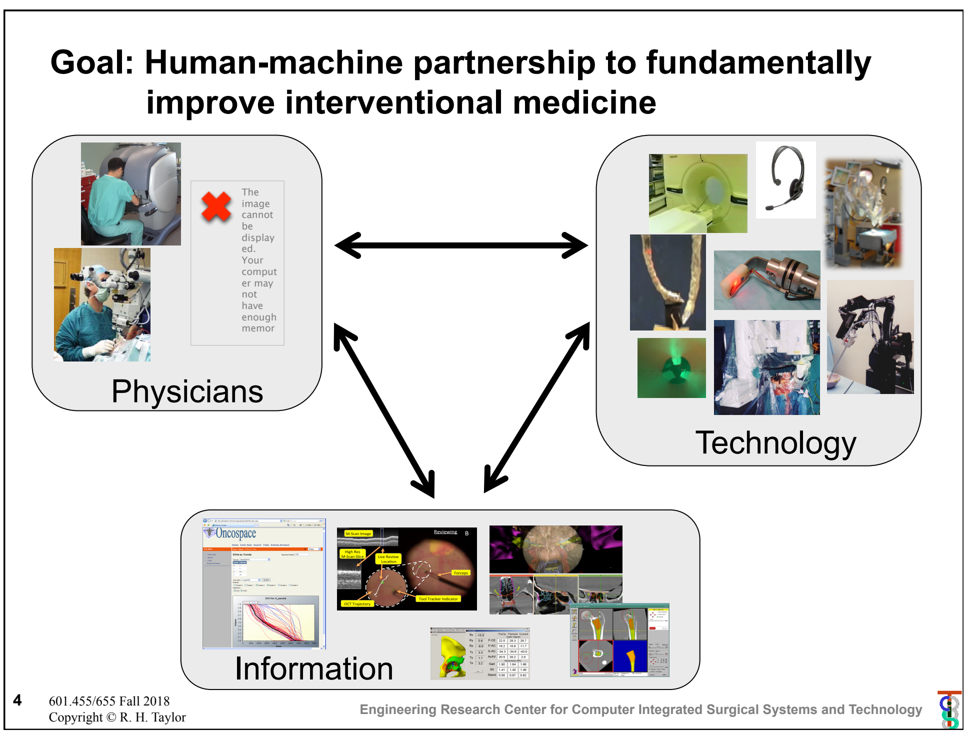
Goal: Human-machine partnership to fundamentally improve interventional medicine
The image cannot be displayed. Your computer may not have enough memor
Physicians
Technology
Information
4
601.455/655 Fall 2018
Copyright © R. H. Taylor
Engineering Research Center for Computer Integrated Surgical Systems and Technology

Complementary Capabilities

Humans	Robots
• Excellent judgment & reasoning	• No judgment
• Excellent optical vision	• Limited vision processing
• Cannot see through tissue	• Can use x-rays, other sensors
• Do not tolerate ionizing radiation	• Do not mind radiation
• Limited precision, hand tremor	• High precision
• No stereotactic accuracy	• High stereotactic accuracy
• Moderately strong	• Variable strength
• High dexterity ("human" scale)	• Dexterity at different scales
• Big hands and bodies	• Variable sizes
• Reasonable force sensitivity	• Can sense very small forces
• Must rely on memory of preoperative plans and data	• Can be programmed to use preoperative plans and data

Common classes of medical robots

- **Surgical "CAD/CAM" systems**
  - Goal is accurate execution of surgical plans
  - Typically based on medical images
  - Planning may be "online" or "offline"
  - Execution is often at least semi-autonomous but may still involve interaction with humans
  - Examples: Orthopaedic robots, needle placement robots, radiation therapy robots
- **Surgical "assistant" systems**
  - Emphasis is on interactive control by human
  - Human input may be through hand controllers (e.g., da Vinci), hand-over-hand (e.g., Mako, JHU "steady hand" robots)
  - Typically augmenting or supplementing human ability
  - Common applications include MIS, microsurgery
- **Note that the distinction is really somewhat arbitrary**
  - Most real systems have aspects of both.

Surgical CAD/CAM: Orthopaedic Robots

Robodoc

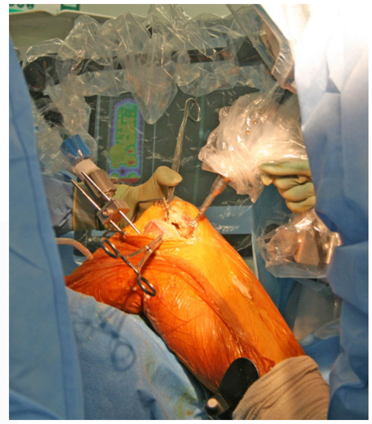

Blue Belt Technologies

D. Glozman
& M. Shoham

ACROBOT surgical robot

Mako Robotics Rio
http://www.makosurgical.com/

Image-guided needle placement

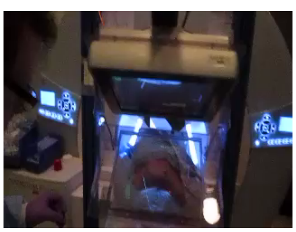

Masamune, Fichtinger, Iordachita, …

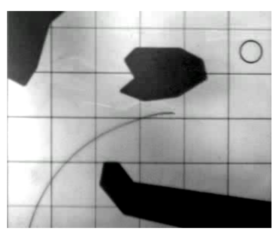

Okamura, Webster, …

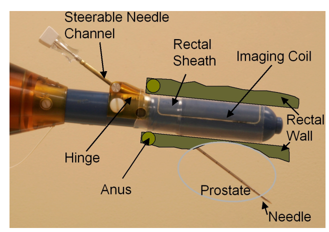

Krieger, Fichtinger, Whitcomb, …

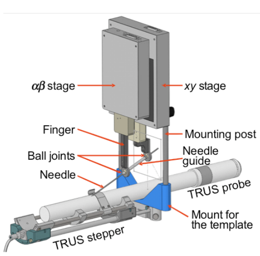

Fichtinger, Kazanzides,Burdette, Song …

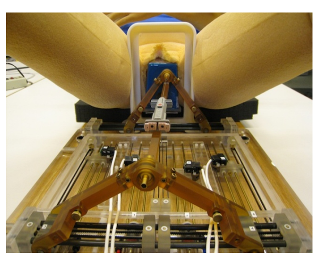

Iordachita, Fischer, Hata…

Taylor, Masamune, Susil, Patriciu, Stoianovici,…

Image Guided Radiotherapy

- Radiation source mounted on robotic arm
- Automatic segmentation of targets
- Automated planning radiation beam path
- Image guide patient motion compensation for more accurate radiation targeting

Cyberknife

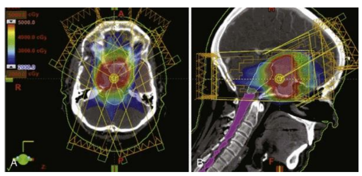

Varian Trilogy System

Slide credit: Howie Choset + RHT

http://www.varian.com/us/oncology/radiation_oncology/trilogy/

Common classes of medical robots

- Surgical "CAD/CAM" systems
  - Goal is accurate execution of surgical plans
  - Typically based on medical images
  - Planning may be "online" or "offline"
  - Execution is often at least semi-autonomous but may still involve interaction with humans
  - Examples: Orthopaedic robots, needle placement robots, radiation therapy robots
- **Surgical "assistant" systems**
  - Emphasis is on interactive control by human
  - Human input may be through hand controllers (e.g., da Vinci), hand-over-hand (e.g., Mako, JHU "steady hand" robots), mouse, or other
  - Typically augmenting or supplementing human ability
  - Common applications include MIS, microsurgery
- Note that the distinction is really somewhat arbitrary
  - Most real systems have aspects of both

MIS Landscape

Intracavity Space

Laparoscopy
Arthroscopy
Pericardioscopy
Thoracoscopy

Superficial

Deep in Anatomy

Tracheoscopy
Cystoscopy
Colposcopy
Laryngoscopy

ERCP

Bronchoscopy
Proctoscopy
Gastroscopy

Intraluminal Pathways

Slide credit: Howie Choset + RHT

Precision Augmentation

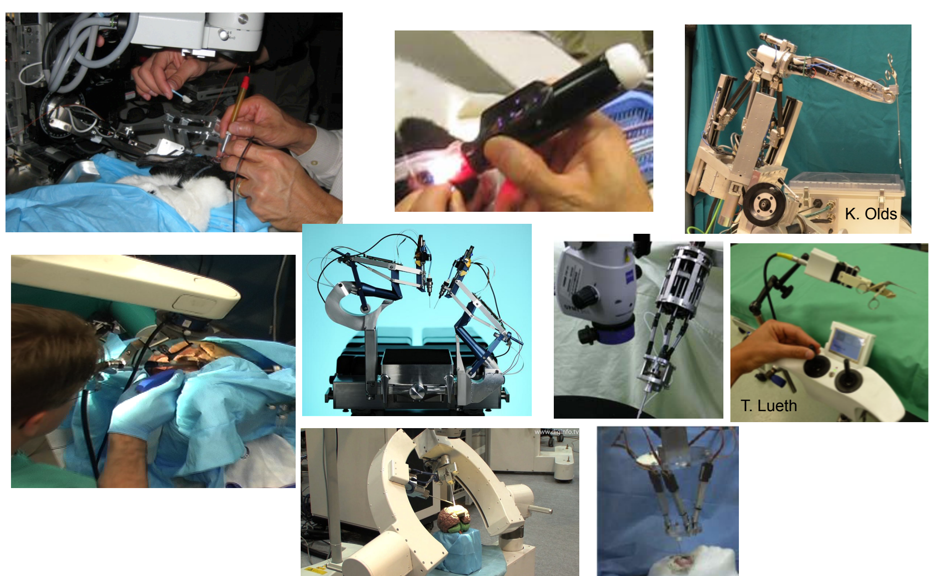

Common classes of medical robots

- **Surgical "CAD/CAM" systems**
  - Goal is accurate execution of surgical plans
  - Typically based on medical images
  - Planning may be "online" or "offline"
  - Execution is often at least semi-autonomous but may still involve interaction with humans
  - Examples: Orthopaedic robots, needle placement robots, radiation therapy robots
- **Surgical "assistant" systems**
  - Emphasis is on interactive control by human
  - Human input may be through hand controllers (e.g., da Vinci), hand-over-hand (e.g., Mako, JHU "steady hand" robots)
  - Typically augmenting or supplementing human ability
  - Common applications include MIS, microsurgery
- **Note that the distinction is really somewhat arbitrary**
  - Most real systems have aspects of both.

Surgical Assistant Systems

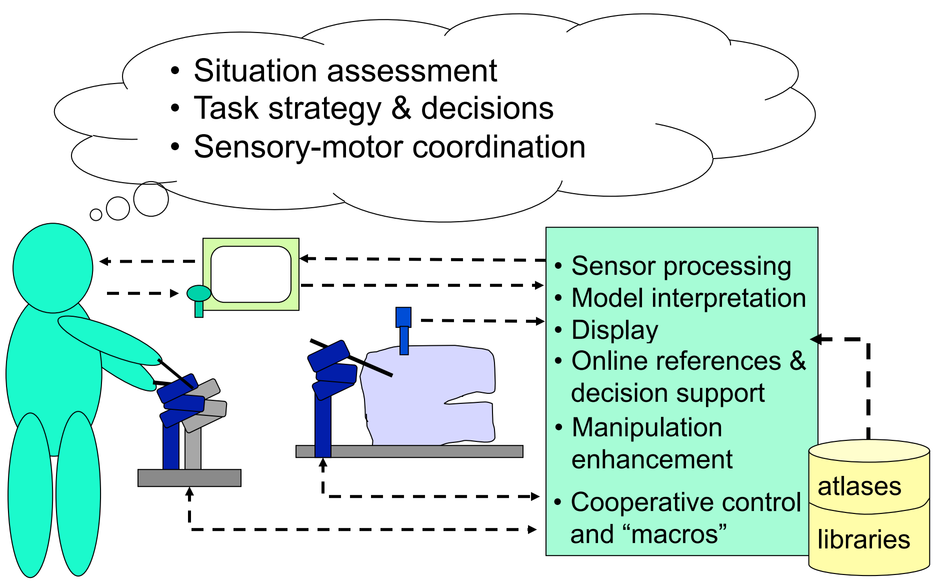

Surgical Assistant Systems

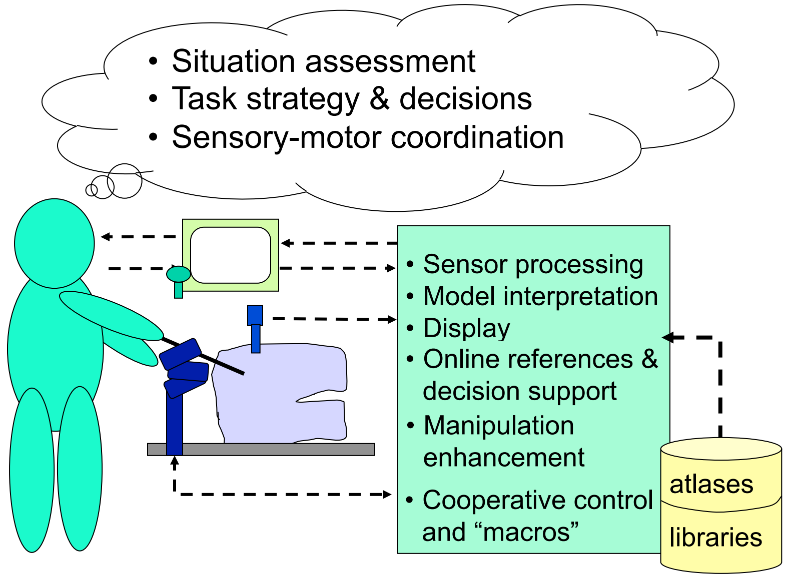

Surgical Assistant Systems

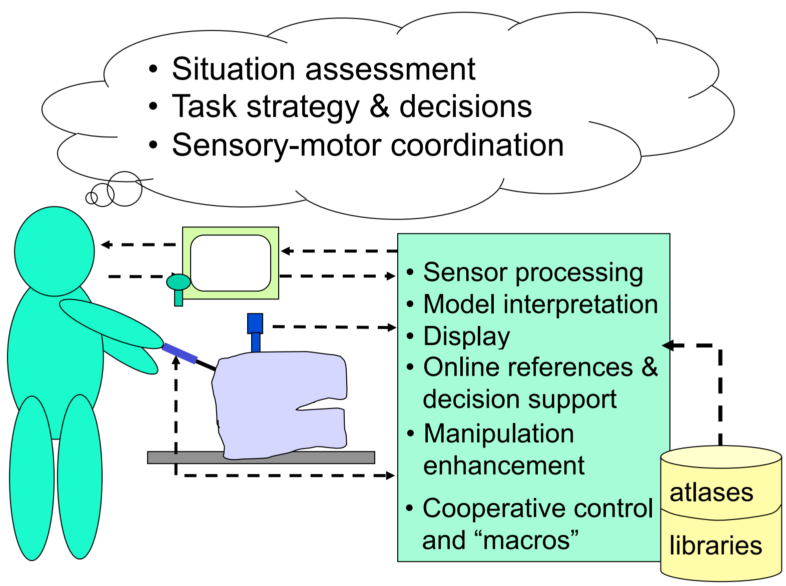

Problem: specifying motion for a [medical] robot

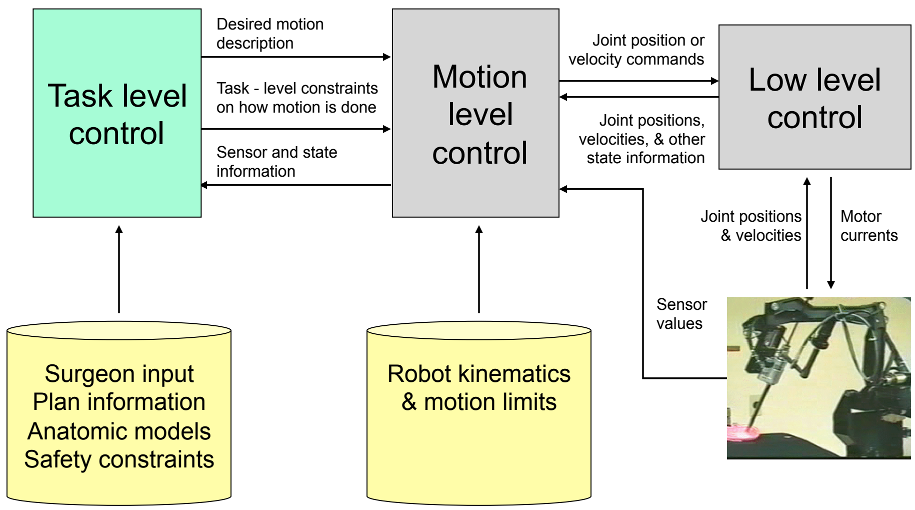

One implementation

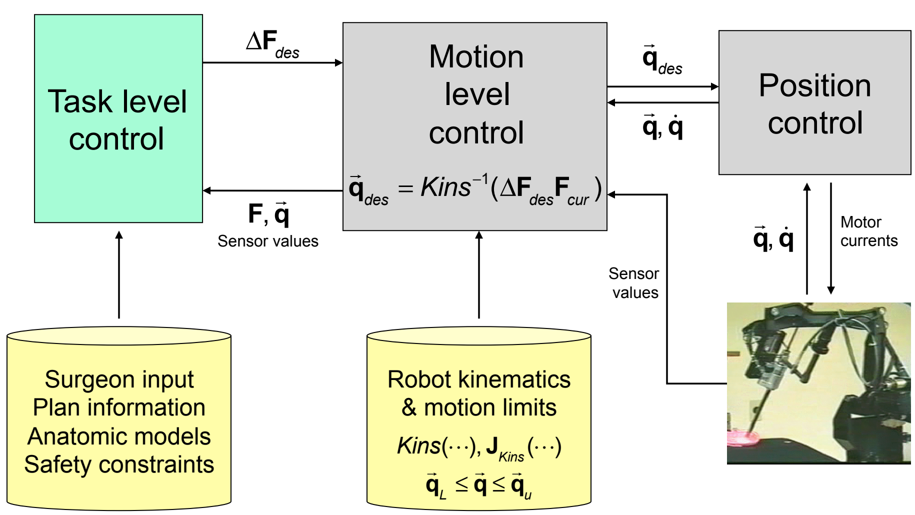

Background: Jacobean Robot Motion Control

Let $\mathbf{F}=[\mathbf{R},\vec{\mathbf{p}}]$ be the current pose of a robot end effector and $\vec{\mathbf{q}}=[q_1,\cdots,q_N]$ be the current joint position values corresponding to $\mathbf{F}$. I.e., $\mathbf{F}=Kins(\vec{\mathbf{q}})$, where $Kins(\cdots)$ is a function computing the "forward kinematics" of the robot.

$$\text{Joint positions } \vec{\mathbf{q}} \longrightarrow \qquad \longrightarrow \text{Pose } \mathbf{F}=kins(\vec{\mathbf{q}})$$

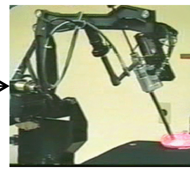

$$\text{Pose } \mathbf{F}(\vec{\mathbf{q}}+\Delta\vec{\mathbf{q}}) = kins(\vec{\mathbf{q}}+\Delta\vec{\mathbf{q}})$$

$$\Delta\mathbf{F}\bullet\mathbf{F} = kins(\vec{\mathbf{q}}+\Delta\vec{\mathbf{q}})$$

$$\Delta\mathbf{F} = kins(\vec{\mathbf{q}}+\Delta\vec{\mathbf{q}})\,kins(\vec{\mathbf{q}})^{-1}$$

Background: Jacobean Robot Motion Control

Let $\mathbf{F}=[\mathbf{R},\vec{\mathbf{p}}]$ be the current pose of a robot end effector and $\vec{\mathbf{q}}=[q_1,\cdots,q_N]$ be the current joint position values corresponding to $\mathbf{F}$. I.e., $\mathbf{F}=Kins(\vec{\mathbf{q}})$, where $Kins(\cdots)$ is a function computing the "forward kinematics" of the robot. Let $\Delta\mathbf{F}\bullet\mathbf{F}=Kins(\vec{\mathbf{q}}+\Delta\vec{\mathbf{q}})$

For small $\Delta\vec{\mathbf{q}}$, we can write the following expression for $\Delta\mathbf{F}=[Rot(\vec{\alpha}),\vec{\varepsilon}]$

$$\Delta\mathbf{F} = Kins(\vec{\mathbf{q}}+\Delta\vec{\mathbf{q}})Kins(\vec{\mathbf{q}})^{-1}$$

which we typically linearize as

$$\Delta\vec{\mathbf{x}} = \begin{bmatrix} \vec{\alpha} \\ \vec{\varepsilon} \end{bmatrix} \approx \mathbf{J}_{Kins}(\vec{\mathbf{q}})\Delta\vec{\mathbf{q}}$$

$$\Delta\vec{\mathbf{q}} \longrightarrow \qquad \longrightarrow \Delta\vec{\mathbf{x}}$$

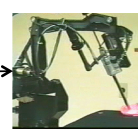

Note that here we are computing $\Delta\mathbf{F}$ in the base frame of the robot. If we want to compute $\Delta\mathbf{F}$ in the end effector frame, so that $\mathbf{F}\bullet\Delta\mathbf{F}=Kins(\vec{\mathbf{q}}+\Delta\vec{\mathbf{q}})$, then we will get a slightly different expression for $\mathbf{J}_{Kins}(\vec{\mathbf{q}})$, though the flavor will be the same

Background: Jacobean Robot Motion Control

Joint positions $\vec{\mathbf{q}}$

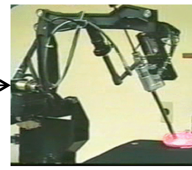

Pose $\mathbf{F} = kins(\vec{\mathbf{q}})$

$$\text{Pose } \mathbf{F}(\vec{\mathbf{q}} + \Delta\vec{\mathbf{q}}) = kins(\vec{\mathbf{q}} + \Delta\vec{\mathbf{q}})$$

$$\Delta\mathbf{F} \bullet \mathbf{F} = kins(\vec{\mathbf{q}} + \Delta\vec{\mathbf{q}})$$

$$\Delta\mathbf{F} = kins(\vec{\mathbf{q}} + \Delta\vec{\mathbf{q}})\, kins(\vec{\mathbf{q}})^{-1}$$

$$\begin{bmatrix} \vec{\alpha} \\ \varepsilon \end{bmatrix} \approx \mathbf{J}(\vec{\mathbf{q}})\Delta\vec{\mathbf{q}}$$

$$\Delta\vec{\mathbf{q}} \approx \mathbf{J}(\vec{\mathbf{q}})^{-1} \begin{bmatrix} \vec{\alpha} \\ \varepsilon \end{bmatrix}$$

Jacobean motion control implementation

Task level control

$\Delta\vec{\mathbf{x}}_{des}$

Motion level control

$\vec{\mathbf{q}}_{des} = \vec{\mathbf{q}} + \mathbf{J}^{-1}(\vec{\mathbf{q}})\Delta\vec{\mathbf{x}}_{des}$

$\vec{\mathbf{q}}_{des}$

$\vec{\mathbf{q}}, \dot{\vec{\mathbf{q}}}$

Position control

$\mathbf{F}, \vec{\mathbf{q}}$

Sensor values

$\vec{\mathbf{q}}, \dot{\vec{\mathbf{q}}}$

Motor currents

Sensor values

Surgeon input
Plan information
Anatomic models
Safety constraints

Robot kinematics
& motion limits
$Kins(\cdots), \mathbf{J}_{Kins}(\cdots)$
$\vec{\mathbf{q}}_L \le \vec{\mathbf{q}} \le \vec{\mathbf{q}}_u$

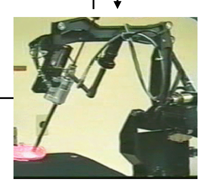

What about parallel-link robots?

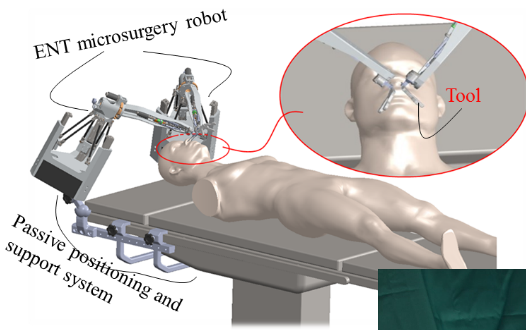

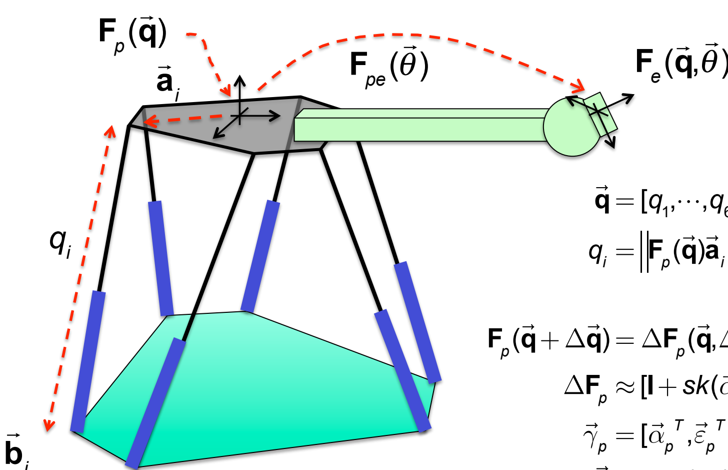

$$\vec{\mathbf{q}} = [q_1,\cdots,q_6]^T = invk(\mathbf{F}_p)$$
$$q_i = \left\|\mathbf{F}_p(\vec{\mathbf{q}})\vec{\mathbf{a}}_i - \mathbf{b}_i\right\|$$

$$\mathbf{F}_p(\vec{\mathbf{q}}+\Delta\vec{\mathbf{q}}) = \Delta\mathbf{F}_p(\vec{\mathbf{q}},\Delta\vec{\mathbf{q}})\mathbf{F}_p(\vec{\mathbf{q}})$$
$$\Delta\mathbf{F}_p \approx [\mathbf{I}+sk(\vec{\alpha}_p),\vec{\varepsilon}_p]$$
$$\vec{\gamma}_p = [\vec{\alpha}_p{}^T,\vec{\varepsilon}_p{}^T]^T$$
$$\Delta\vec{\mathbf{q}} \approx \mathbf{J}_{invk}(\mathbf{F}_p(\vec{\mathbf{q}}))\vec{\gamma}_p$$
$$\vec{\gamma}_p \approx \mathbf{J}_{invk}(\mathbf{F}_p(\vec{\mathbf{q}}))^{-1}\Delta\vec{\mathbf{q}}$$

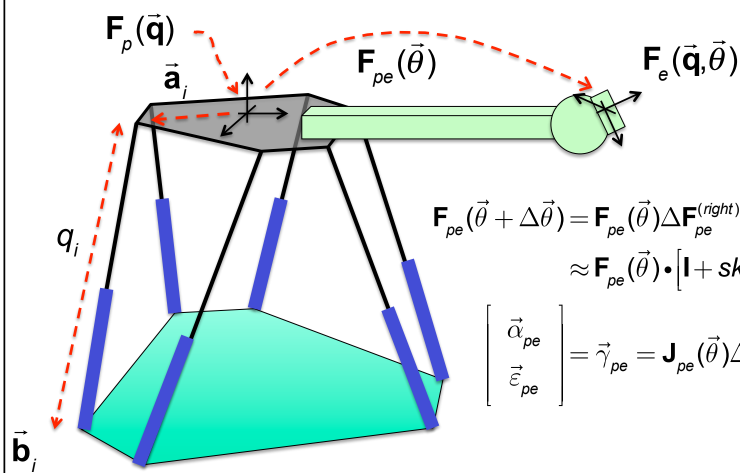

$$\mathbf{F}_{pe}(\vec{\theta}+\Delta\vec{\theta}) = \mathbf{F}_{pe}(\vec{\theta})\Delta\mathbf{F}_{pe}^{(right)}(\vec{\theta},\Delta\vec{\theta})$$

$$\approx \mathbf{F}_{pe}(\vec{\theta})\bullet\left[\mathbf{I}+sk(\vec{\alpha}_{pe}),\vec{\varepsilon}_{pe}\right]$$

$$\begin{bmatrix}\vec{\alpha}_{pe}\\ \vec{\varepsilon}_{pe}\end{bmatrix} = \vec{\gamma}_{pe} = \mathbf{J}_{pe}(\vec{\theta})\Delta\vec{\theta} = \begin{bmatrix}\mathbf{J}_{pe}^{\mathbf{R}}(\vec{\theta})\\ \mathbf{J}_{pe}^{\vec{\mathbf{p}}}(\vec{\theta})\end{bmatrix}\Delta\vec{\theta}$$

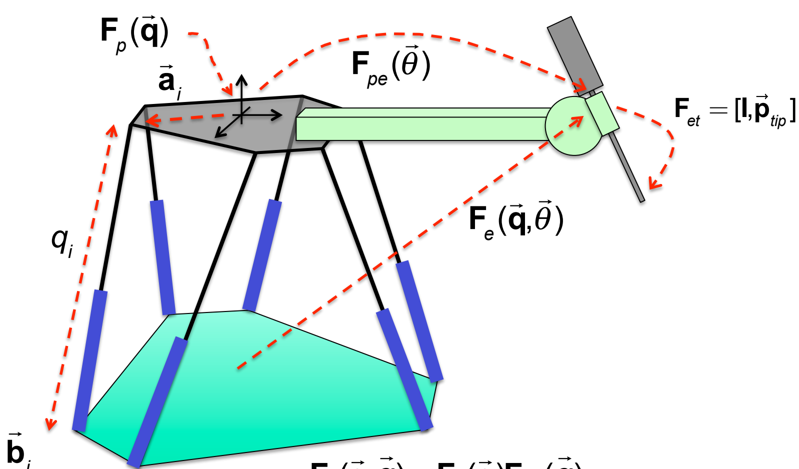

$$\mathbf{F}_e(\vec{\mathbf{q}},\vec{q}) = \mathbf{F}_p(\vec{\mathbf{q}})\mathbf{F}_{pe}(\vec{q})$$

$$\mathbf{F}_e(\vec{\mathbf{q}}+\Delta\vec{\mathbf{q}},\vec{q}+\Delta\vec{q}) = \Delta\mathbf{F}_p(\vec{\mathbf{q}},\Delta\vec{\mathbf{q}})\mathbf{F}_p(\vec{\mathbf{q}})\mathbf{F}_{pe}(\vec{q}+\Delta\vec{q})$$

Steady Hand Robot

Hands on compliance control

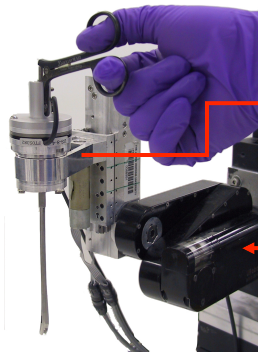

Handle Force

K_v

$$\dot{\vec{\mathbf{x}}}_{des} = \mathbf{K}_v \vec{\mathbf{f}}_h$$
$$\dot{\mathbf{q}}_{cmd} = \mathbf{J}^{-1}_{kins} \dot{\vec{\mathbf{x}}}_{des}$$

Joint Velocities

[1] R. H. Taylor, J. Funda, B. Eldgridge, S. Gomory, K. Gruben, D. LaRose, M. Talamini, L. Kavoussi, and J. anderson, "Telerobotic assistant for laparoscopic surgery.", IEEE Eng Med Biol, vol. 14- 3, pp. 279-288, 1995

[2] R. Taylor, P. Jensen, L. Whitcomb, A. Barnes, R. Kumar, D. Stoianovici, P. Gupta, Z. Wang, E. deJuan, and L. Kavoussi, "A Steady-Hand Robotic System for Microsurgical Augmentation", International Journal of Robotics Research, vol. 18- 12, pp. 1201-1210, 1999

Steady Hand Robot

Hands on compliance control with force scaling

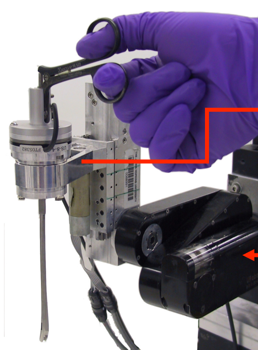

Handle Force

K_v

$$\dot{\vec{\mathbf{x}}}_{des} = \mathbf{K}_v (\vec{\mathbf{f}}_h - \gamma \vec{\mathbf{f}}_{tip})$$
$$\dot{\mathbf{q}}_{cmd} = \mathbf{J}^{-1}_{kins} \dot{\vec{\mathbf{x}}}_{des}$$

Joint Velocities

Tool tip Force

[1] D. Rothbaum, J. Roy, G. Hager, R. Taylor, and L. Whitcomb, "Task Performance in stapedotomy: Comparison between surgeons of different experience levels", Otolaryngology -- Head and Neck Surgery, vol. 128- 1, pp. 71-77, January 2003

[2] J. Roy and L. L. Whitcomb, "Adaptive Force Control of Position Controlled Robots: Theory and Experiment", IEEE Transactions on Robotics and Automation, vol. 18- 2, pp. 121-137, April 2002

Steady Hand Robot (Alternative Formulation)

Hands on compliance control with force scaling

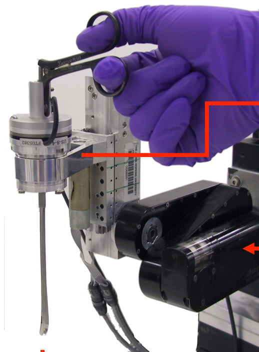

Handle Force

K_v

$$\vec{\dot{\mathbf{x}}}_{des} = \mathbf{K}_v(\vec{\mathbf{f}}_h - \gamma \vec{\mathbf{f}}_{tip})$$

$$\vec{\dot{\mathbf{q}}}_{cmd} = \underset{\vec{\dot{\mathbf{q}}}_{cmd}}{\arg\min} \left\| \vec{\dot{\mathbf{x}}}_{des} - \mathbf{J}_{kins}\vec{\dot{\mathbf{q}}}_{cmd} \right\|$$

Joint Velocities

Tool tip Force

[1] D. Rothbaum, J. Roy, G. Hager, R. Taylor, and L. Whitcomb, "Task Performance in stapedotomy: Comparison between surgeons of different experience levels", Otolaryngology -- Head and Neck Surgery, vol. 128- 1, pp. 71-77, January 2003
[2] J. Roy and L. L. Whitcomb, "Adaptive Force Control of Position Controlled Robots: Theory and Experiment", IEEE Transactions on Robotics and Automation, vol. 18- 2, pp. 121-137, April 2002

Example: Fenestratration of Stapes Footplate

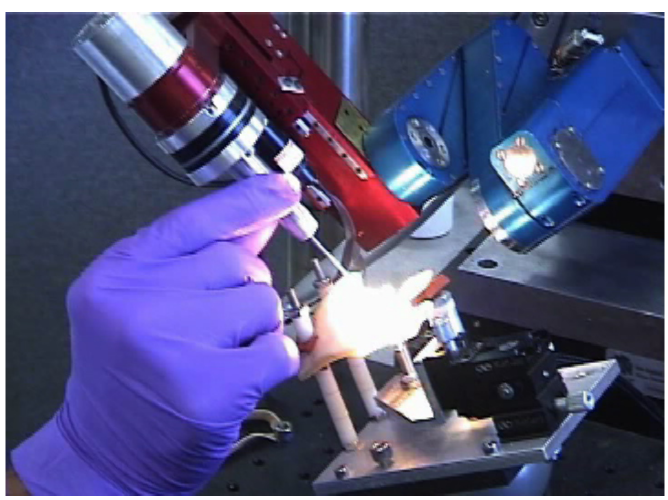

Example: Fenestratration of Stapes Footplate

Virtual Fixtures

- Bridge the gap between autonomous robots and direct human control.
- Assist the human operator in safer, faster, and more accurate task completion.

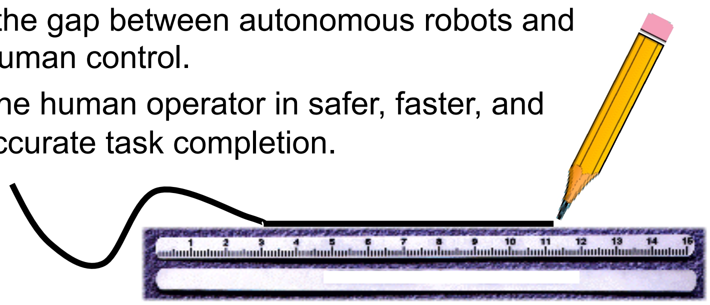

- Broadly Categorized
  - Guidance VF
  - Forbidden Region VF
- Different implementation
  - Tele-manipulation
  - Cooperative Control

Background: Virtual Fixtures

- First proposed for complex telerobotic tasks, but draw upon rich prior research in robot assembly and other manufacturing automation applications
- Many authors, e.g.,
  - L. B. Rosenberg, "Virtual Fixtures: Perceptual Tools for Telerobotic Manipulation," *Proc. IEEE Virtual Reality International Symposium,* 1993.
  - B. Davies, S. Harris, M. Jakopec, K. Fan, and J. cobb, "Intraoperative application of a robotic knee surgery system", *MICCAI* 1999.
  - S. Park, R. D. Howe, and D. F. Torchiana, "Virtual Fixtures for Robotic Cardiac Surgery", *MICCAI* 2001.
  - S. Payandeh and Z. Stanisic, "On Application of Virtual Fixtures as an Aid for Telemanipulation and Training," *Symposium on Haptic Interfaces for Virtual Environment and Teleoperator Systems*, 2002.
- Discussion that follows draws upon work at IBM Research and within the CISST ERC at JHU. E.g.,
  - Funda, R. Taylor, B. Eldridge, S. Gomory, and K. Gruben, "Constrained Cartesian motion control for teleoperated surgical robots," *IEEE Transactions on Robotics and Automation,* vol. 12, pp. 453-466, 1996.
  - R. Kumar, An Augmented Steady Hand System for Precise Micromanipulation, Ph.D thesis in Computer Science, The Johns Hopkins University, Baltimore, 2001.
  - M. Li, M. Ishii, and R. H. Taylor, "Spatial Motion Constraints in Medical Robot Using Virtual Fixtures Generated by Anatomy," *IEEE Transactions on Robotics*, vol. 2, pp. 1270-1275, 2006.
  - A. Kapoor, M. Li, and R. H. Taylor "Constrained Control for Surgical Assistant Robots," in *IEEE Int. Conference on Robotics and Automation*, Orlando, 2006, pp. 231-236.
  - A. Kapoor and R. Taylor, "A Constrained Optimization Approach to Virtual Fixtures for Multi-Handed Tasks," in IEEE International Conference on Robotics and Automation (ICRA), Pasadena, 2008, pp. 3401-3406.
  - M. Li, *Intelligent Robotic Surgical Assistance for Sinus Surgery*, PhD Thesis in Computer Science Baltimore, Maryland: The Johns Hopkins University, 2005.
  - Ankur Kapoor, *Motion Constrained Control of Robots for Dexterous Surgical Tasks*, Ph.D. Thesis in Computer Science, The Johns Hopkins University, Baltimore, September 2007

Original Motivation for IBM Work

- Kinematic control of robots for MIS
- E.g., LARS and HISAR robots
- LARS and other IBM robots were kinematically redundant
  - Typically 7-9 actuated joints
- But tasks often imposed kinematic constraints
  - E.g., no lateral motion at trocar
- Some robots (e.g., IBM/JHU HISAR and CMI's AESOP) had passive joints
- General goals
  - Exploit redundancy in best way possible
  - Come as close as possible to providing desired motion subject to robot and task limits
- **Our approach:** view this as a constrained optimization problem

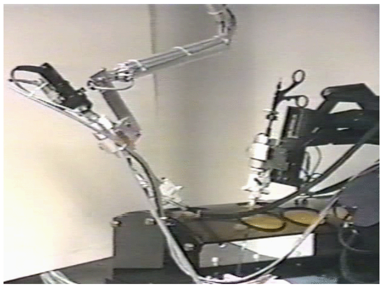

LARS degrees of freedom

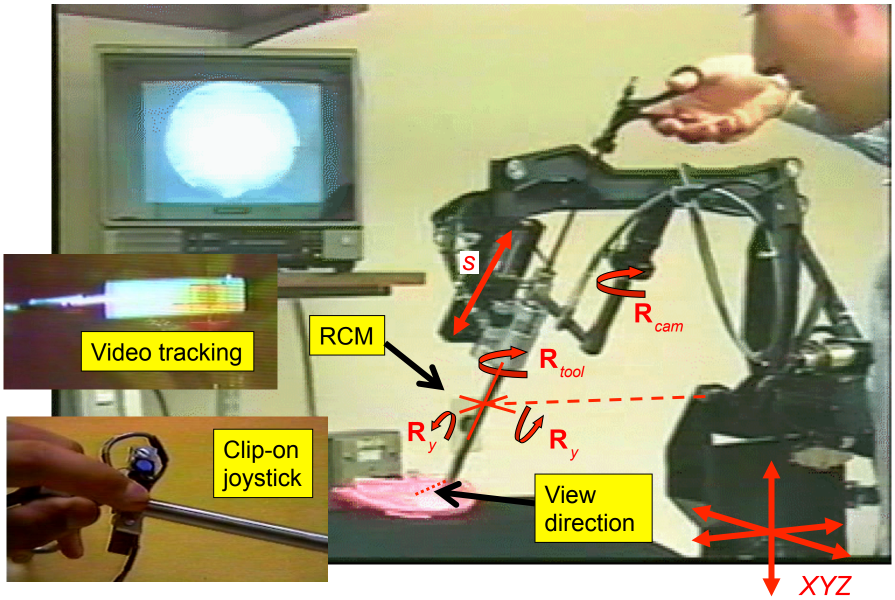

LARS Video

LARS Video

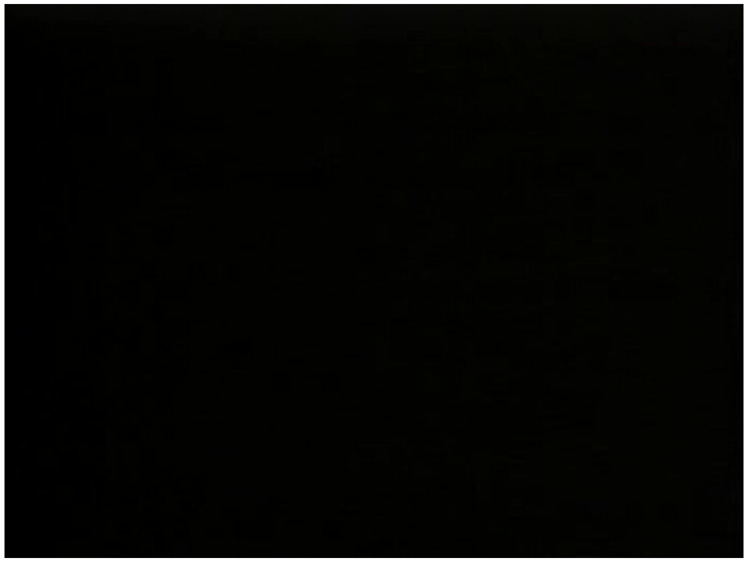

Motion Specification Problem

- **Requirements**
  – The tool shaft must pass within a specified distance of the entry port into the patient's body
  – The individual joint limits may not be exceeded
- **Goals**
  – Aim the camera as close as possible at a target
    - ***or*** move view in direction indicated by clip-on pointing device
    - ***or*** move to track a video target on an instrument
    - ***or*** aim the working channel of the endoscope at a target
    - ***or*** something else (maybe a combination of goals)
  – Keep the view as "upright" as possible
  – Tool should pass as close as possible to entry port center
  – Keep joints far away from their limits, to preserve options for future motion
  – Minimize motion of XYZ joints
  – *Etc.*

Our approach: view as an optimization problem

- Currently formulate problem as constrained least squares problem
- Express goals in the objective function
- If multiple goals, objective function is a weighted sum of individual elements
- Add constraints for requirements
- Express constraints and objective function terms in whatever coordinate system is convenient
- Use Jacobean formulation to transform to joint space
- Solve for joint motion

Example: keep tool tip near a point

$$\vec{D}(\Delta\vec{\mathbf{x}}) = \Delta\mathbf{F}(\vec{\mathbf{q}},\Delta\vec{\mathbf{q}}) \bullet \mathbf{F} \bullet \mathbf{p}_{tip} - \vec{\mathbf{p}}_{goal}$$
$$= \vec{\alpha} \times \vec{\mathbf{t}} + \vec{\varepsilon} + \vec{\mathbf{t}} - \vec{\mathbf{p}}_{goal} \quad \text{where } \vec{\mathbf{t}} = \mathbf{F} \bullet \mathbf{p}_{tip}$$
$$\vec{\alpha} = \mathbf{J}_{\vec{\alpha}}(\vec{\mathbf{q}})\Delta\vec{\mathbf{q}}$$
$$\vec{\varepsilon} = \mathbf{J}_{\vec{\varepsilon}}(\vec{\mathbf{q}})\Delta\vec{\mathbf{q}}$$

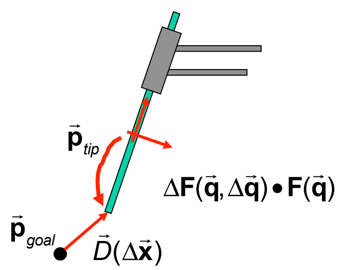

Suppose we want to stay as close as possible while never going beyond 3mm from goal and also obeying joint limits

$$\Delta\mathbf{q}_{des} = \underset{\Delta\vec{\mathbf{q}}}{\arg\min} \left\|\vec{D}(\Delta\vec{\mathbf{x}})\right\|^2 = \left\|\vec{\alpha} \times \vec{\mathbf{t}} + \vec{\varepsilon} + \vec{\mathbf{t}} - \vec{\mathbf{p}}_{goal}\right\|^2$$

Subject to

$$\vec{\alpha} = \mathbf{J}_{\vec{\alpha}}(\vec{\mathbf{q}})\Delta\vec{\mathbf{q}}$$
$$\vec{\varepsilon} = \mathbf{J}_{\vec{\varepsilon}}(\vec{\mathbf{q}})\Delta\vec{\mathbf{q}}$$
$$\left\|\vec{\alpha} \times \vec{\mathbf{t}} + \vec{\varepsilon} + \vec{\mathbf{t}} - \vec{\mathbf{p}}_{goal}\right\| \le 3$$
$$\vec{\mathbf{q}}_L - \vec{\mathbf{q}} \le \Delta\vec{\mathbf{q}} \le \vec{\mathbf{q}}_U - \vec{\mathbf{q}}$$

Example: keep tool tip near a point

Suppose we want to stay as close as possible while never going beyond 3mm from goal and also obeying joint limits, but we also want to minimize the change in direction of the tool shaft

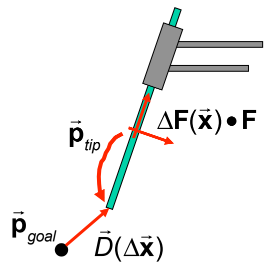

$$\Delta\mathbf{q}_{des} = \arg\min_{\Delta\vec{\mathbf{q}}} \ \zeta \left\|\vec{\mathrm{D}}(\Delta\vec{\mathbf{x}})\right\|^2 + \eta \ \left\|\alpha \times \mathbf{R} \bullet \vec{\mathbf{z}}\right\|^2$$

Subject to

$$\vec{\mathbf{x}} = \mathbf{F} \bullet \vec{\mathbf{p}}_{tip}$$

$$\vec{\mathrm{D}}(\Delta\vec{\mathbf{x}}) = \vec{\alpha} \times \vec{\mathbf{t}} + \vec{\varepsilon} + \vec{\mathbf{x}} - \vec{\mathbf{p}}_{goal}$$

$$\vec{\alpha} = \mathbf{J}_{\vec{\alpha}}(\vec{\mathbf{q}})\Delta\vec{\mathbf{q}} \ ; \ \ \vec{\varepsilon} = \mathbf{J}_{\vec{\varepsilon}}(\vec{\mathbf{q}})\Delta\vec{\mathbf{q}}$$

$$\left\|\vec{\mathrm{D}}(\Delta\vec{\mathbf{x}})\right\| \le 3$$

$$\vec{\mathbf{q}}_L - \vec{\mathbf{q}} \le \Delta\vec{\mathbf{q}} \le \vec{\mathbf{q}}_U - \vec{\mathbf{q}}$$

Note weighting factors

$$\vec{\mathbf{x}} = \mathbf{F} \bullet \vec{\mathbf{p}}_{tip}$$

Solving the optimization problem

- **Constrained linear least squares**
  - Combine constraints and goals from task and robot control
  - Linearize and constrained least squares problem

$$\Delta\vec{\mathbf{q}}_{des} = \arg\min_{\Delta\vec{\mathbf{q}}} \left\|\mathbf{E}_{task}\Delta\vec{\mathbf{x}} - \vec{\mathbf{f}}_{task}\right\|^2 + \left\|\mathbf{E}_{\vec{\mathbf{q}}}\Delta\vec{\mathbf{x}} - \vec{\mathbf{f}}_{\vec{\mathbf{q}}}\right\|^2$$

subject to

$$\Delta\vec{\mathbf{x}} = \mathbf{J}\Delta\vec{\mathbf{q}}; \ \ \mathbf{A}_{task}\Delta\vec{\mathbf{x}} \le \vec{\mathbf{b}}_{task} \ \ ; \mathbf{A}_{\vec{\mathbf{q}}}\Delta\vec{\mathbf{q}} \le \vec{\mathbf{b}}_{\vec{\mathbf{q}}}$$

  - E.g., using “non-negative least squares” methods developed by Lawson and Hanson
  - Approach used in our IBM work and in Kumar, Li, Kapoor theses
- **Constrained nonlinear least squares**
  - Approach explored by Kapoor (discuss later)
- **Can also minimize other objective functions**
  - E.g., minimize an L1 norm (linear programming problem)

Linear least squares implementation

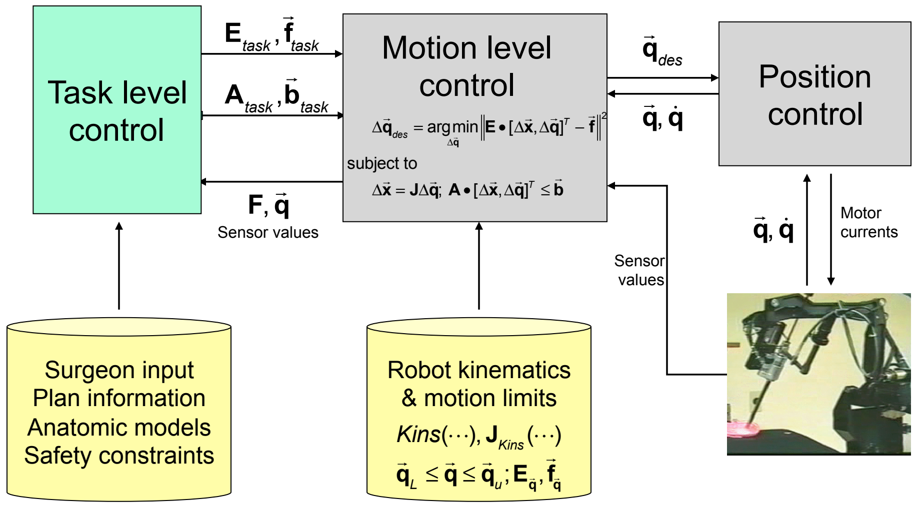

Some IBM Movies

Early Constrained Motion System (LapSYS)

Vision-guided targeting

Steady Hand Robot

High Level Constrained Control

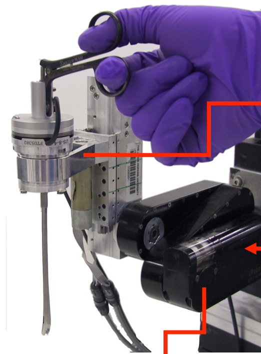

Handle Force → K_v → Optimization Framework

Optimization Framework → Joint Velocities

Current Frame(s) Info. → Geometric Constraints on Frame(s) → Optimization Framework

Reference Direction → Geometric Constraints on Frame(s)

Example: Hands-on Guiding with Forbidden Half Space

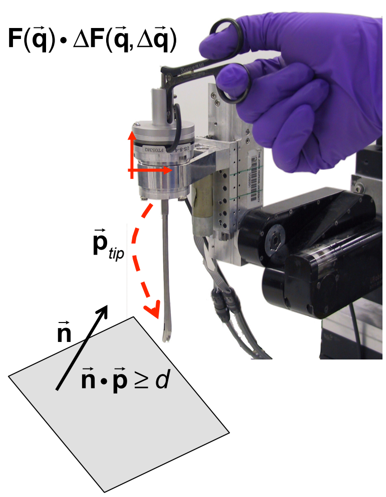

$$\Delta\vec{\mathbf{q}} = \underset{\Delta\vec{\mathbf{q}}}{\arg\min} \left\| \mathbf{K}_v \vec{\mathbf{f}} - \mathbf{J}_{rhs}(\vec{\mathbf{q}}) \Delta\vec{\mathbf{q}} \right\|$$

Such that

$$d \leq \vec{\mathbf{n}} \bullet (\mathbf{F}(\vec{\mathbf{q}}) \Delta\mathbf{F}_{rhs}(\vec{\mathbf{q}},\Delta\vec{\mathbf{q}}) \bullet \vec{\mathbf{p}}_{tip})$$

Note here we are using the right hand side Jacobean, since the force sensor is associated with the tool attachment point, and it is more natural for the motions to comply to pushes on the tool handle.

LHS versus RHS Jacobeans

$$\Delta\mathbf{F}\left(\mathbf{J}_{kins}(\vec{\mathbf{q}})\Delta\vec{\mathbf{q}}\right)\bullet\mathbf{F}(\vec{\mathbf{q}}) = \mathbf{F}(\vec{\mathbf{q}})\bullet\Delta\mathbf{F}(\mathbf{J}_{rhs}(\vec{\mathbf{q}})\Delta\vec{\mathbf{q}})$$
$$\Delta\mathbf{R}\left(\mathbf{J}_{kins}(\vec{\mathbf{q}})\Delta\vec{\mathbf{q}}\right)\bullet\mathbf{R}(\vec{\mathbf{q}}) = \mathbf{R}(\vec{\mathbf{q}})\bullet\Delta\mathbf{R}(\mathbf{J}_{rhs}(\vec{\mathbf{q}})\Delta\vec{\mathbf{q}})$$

Define

$$\mathbf{J}_{kins} = \begin{bmatrix} \mathbf{J}^{\alpha}_{kins} \\ \mathbf{J}^{\varepsilon}_{kins} \end{bmatrix} \quad \vec{\alpha}_{kins} = \mathbf{J}^{\alpha}_{kins}\Delta\vec{\mathbf{q}} \quad \mathbf{J}_{rhs} = \begin{bmatrix} \mathbf{J}^{\alpha}_{rhs} \\ \mathbf{J}^{\varepsilon}_{rhs} \end{bmatrix} \quad \vec{\alpha}_{rhs} = \mathbf{J}^{\alpha}_{rhs}\Delta\vec{\mathbf{q}}$$

so

$$\Delta\mathbf{R}(\mathbf{J}_{rhs}(\vec{\mathbf{q}})\Delta\vec{\mathbf{q}}) = \mathbf{R}(\vec{\mathbf{q}})^{-1}\Delta\mathbf{R}\left(\mathbf{J}_{kins}\Delta\vec{\mathbf{q}}\right)\bullet\mathbf{R}(\vec{\mathbf{q}})$$
$$\mathbf{I} + sk(\alpha_{rhs}) = \mathbf{I} + \mathbf{R}^{-1}sk(\vec{\alpha}_{kins})\mathbf{R}$$
$$sk(\vec{\alpha}_{rhs}) = sk(\mathbf{R}^{-1}\vec{\alpha}_{kins})$$
$$\mathbf{J}^{\alpha}_{rhs} = \mathbf{R}^{-1}\mathbf{J}^{\alpha}_{kins}$$

and one can do something similar for the $\Delta\vec{\mathbf{p}}$ parts (exercise).

Example: Hands-on Guiding with Forbidden Half Space

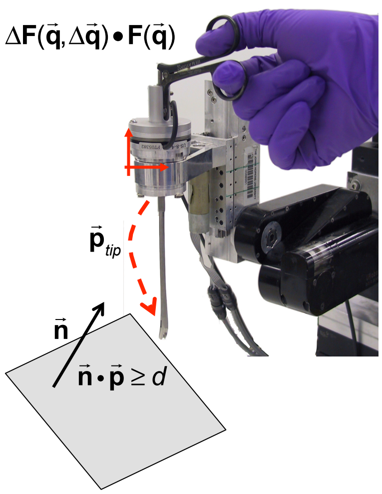

$$\Delta\vec{\mathbf{q}} = \underset{\Delta\vec{\mathbf{q}}}{\arg\min}\left\|\mathbf{K}_v\vec{\mathbf{f}} - \mathbf{J}_{rhs}(\vec{\mathbf{q}})\Delta\vec{\mathbf{q}}\right\|$$

Such that

$$\begin{bmatrix} \vec{\alpha} \\ \vec{\varepsilon} \end{bmatrix} = \mathbf{J}_{rhs}(\vec{\mathbf{q}})\Delta\vec{\mathbf{q}}$$
$$d \le \vec{\mathbf{n}}\bullet\left(\mathbf{F}(\vec{\mathbf{q}})\bullet(\vec{\alpha}\times\vec{\mathbf{p}}_{tip} + \vec{\varepsilon} + \vec{\mathbf{p}}_{tip})\right)$$

I.e.,

$$\begin{bmatrix} \vec{\alpha} \\ \vec{\varepsilon} \end{bmatrix} = \mathbf{J}_{rhs}(\vec{\mathbf{q}})\Delta\vec{\mathbf{q}}$$
$$d \le \vec{\mathbf{n}}\bullet\left(\mathbf{R}(\vec{\mathbf{q}})\bullet(\vec{\alpha}\times\vec{\mathbf{p}}_{tip} + \vec{\varepsilon} + \vec{\mathbf{p}}_{tip}) + \vec{\mathbf{p}}_{kins}\right)$$

Example: Hands-on Guiding with Forbidden Half Space

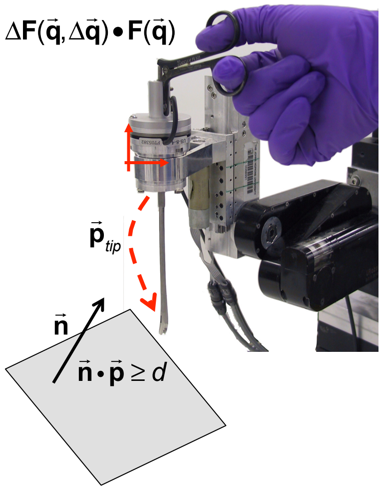

$$\Delta\vec{q} = \underset{\Delta\vec{q}}{\arg\min} \left\| \mathbf{K}_v \vec{f} - \mathbf{J}_{rhs}(\vec{q})\Delta\vec{q} \right\|^2$$

Such that

$$\begin{bmatrix}\vec{\alpha}\\ \vec{\varepsilon}\end{bmatrix} = \mathbf{J}_{rhs}(\vec{q})\Delta\vec{q}$$

$$d - \vec{n}\bullet\vec{x} \leq \vec{n}\bullet\left(\mathbf{R}(\vec{q})\bullet(\vec{\alpha}\times\vec{p}_{tip}+\vec{\varepsilon})\right)$$

$$\vec{x} = \mathbf{F}(\vec{q})\vec{p}_{tip}$$

Example: Hands-on Guiding with Forbidden Half Space

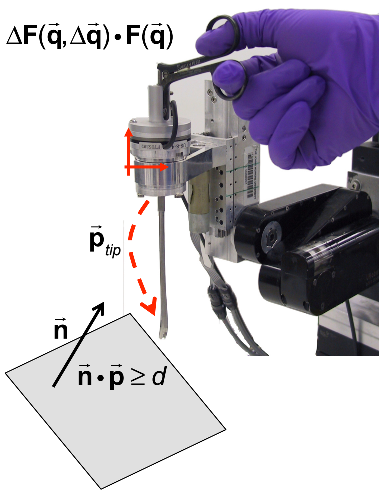

$$\Delta\vec{q} = \underset{\Delta\vec{q}}{\arg\min} \left\| \mathbf{K}_v \vec{f} - \mathbf{J}_{kins}(\vec{q})\Delta\vec{q} \right\|^2$$

Such that

$$d \leq \vec{n}\bullet(\Delta\mathbf{F}(\vec{q},\Delta\vec{q})\bullet\mathbf{F}(\vec{q})\bullet\vec{p}_{tip})$$

If we use the LHS Jacobean, we get something similar. Note however that in this case the gain matrix will likely be pose dependent, since the it is more natural for the surgeon's hand to follow the tool. So it is useful to be able to make the conversion …

Example: Hands-on Guiding to Follow a Path

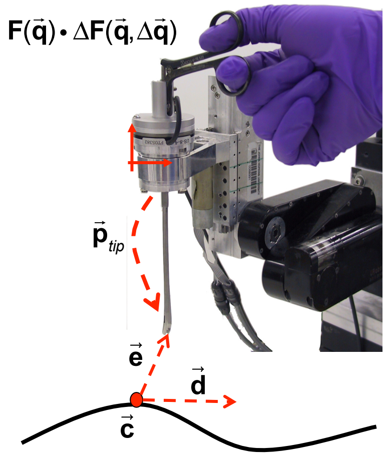

$$\Delta\vec{\mathbf{q}} = \underset{\Delta\vec{\mathbf{q}}}{\arg\min} \left\| \mathbf{K}_v \vec{\mathbf{f}} - \mathbf{J}_{rhs}(\vec{\mathbf{q}}) \Delta\vec{\mathbf{q}} \right\|$$

Such that

$$\vec{\mathbf{e}} = (\mathbf{F}(\vec{\mathbf{q}}) \Delta\mathbf{F}_{rhs}(\vec{\mathbf{q}}, \Delta\vec{\mathbf{q}}) \bullet \vec{\mathbf{p}}_{tip}) - \vec{\mathbf{c}}$$

$$\delta \geq \left\| \vec{\mathbf{e}} - \left(\vec{\mathbf{d}} \bullet \vec{\mathbf{e}} \right) \vec{\mathbf{d}} \right\|$$

Example: Hands-on Guiding to Follow a Path

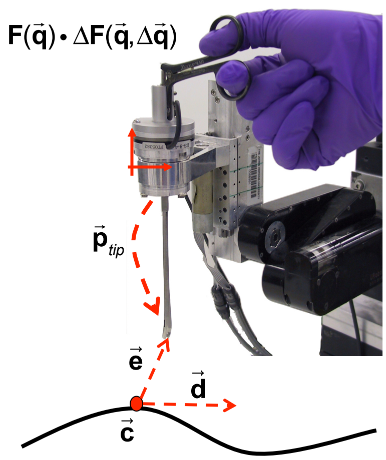

$$\Delta\vec{\mathbf{q}} = \underset{\Delta\vec{\mathbf{q}}}{\arg\min} \left\| \mathbf{K}_v \vec{\mathbf{f}} - \mathbf{J}_{rhs}(\vec{\mathbf{q}}) \Delta\vec{\mathbf{q}} \right\|^2$$

Such that

$$\vec{\mathbf{e}} = (\mathbf{F}(\vec{\mathbf{q}}) \left(\vec{\alpha} \times \vec{\mathbf{p}}_{tip} + \vec{\varepsilon} + \vec{\mathbf{p}}_{tip} \right)) - \vec{\mathbf{c}}$$

$$\begin{bmatrix} \vec{\alpha} \\ \vec{\varepsilon} \end{bmatrix} = \mathbf{J}_{rhs}(\vec{\mathbf{q}}) \Delta\vec{\mathbf{q}}$$

$$\delta \geq \left\| \vec{\mathbf{e}} - \left(\vec{\mathbf{d}} \bullet \vec{\mathbf{e}} \right) \vec{\mathbf{d}} \right\|$$

Example: Hands-on Guiding to Follow a Path

$\mathbf{F}(\vec{\mathbf{q}}) \bullet \Delta\mathbf{F}(\vec{\mathbf{q}},\Delta\vec{\mathbf{q}})$

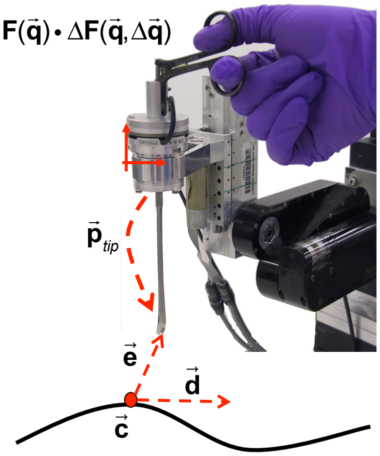

$$\Delta\vec{\mathbf{q}} = \underset{\Delta\vec{\mathbf{q}}}{\arg\min} \left\| \mathbf{K}_v \vec{\mathbf{f}} - \mathbf{J}_{rhs}(\vec{\mathbf{q}})\Delta\vec{\mathbf{q}} \right\|^2$$

Such that

$$\vec{\mathbf{e}} = \mathbf{R}(\vec{\mathbf{q}})\left(\vec{\alpha} \times \vec{\mathbf{p}}_{tip} + \vec{\varepsilon} + \vec{\mathbf{p}}_{tip}\right) + \vec{\mathbf{p}}(\vec{\mathbf{q}}) - \vec{\mathbf{c}}$$

$$\begin{bmatrix} \vec{\alpha} \\ \vec{\varepsilon} \end{bmatrix} = \mathbf{J}_{rhs}(\vec{\mathbf{q}})\Delta\vec{\mathbf{q}}$$

$$\delta \geq \left\| \vec{\mathbf{e}} - \left(\vec{\mathbf{d}} \bullet \vec{\mathbf{e}}\right)\vec{\mathbf{d}} \right\|$$

Example: Hands-on Guiding to Follow a Path

$\mathbf{F}(\vec{\mathbf{q}}) \bullet \Delta\mathbf{F}(\vec{\mathbf{q}},\Delta\vec{\mathbf{q}})$

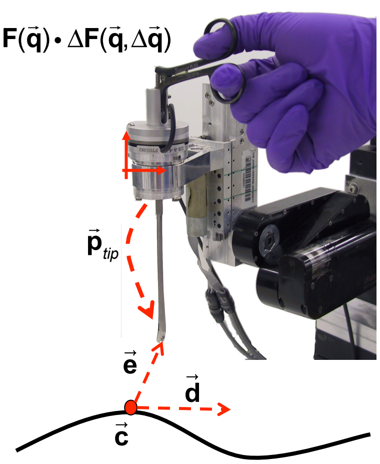

$$\Delta\vec{\mathbf{q}} = \underset{\Delta\vec{\mathbf{q}}}{\arg\min} \left\| \mathbf{K}_v \vec{\mathbf{f}} - \mathbf{J}_{rhs}(\vec{\mathbf{q}})\Delta\vec{\mathbf{q}} \right\|^2$$

Such that

$$\vec{\mathbf{e}} = \vec{\mathbf{p}}(\vec{\mathbf{q}}) + \mathbf{R}(\vec{\mathbf{q}})\vec{\mathbf{p}}_{tip} + \mathbf{R}(\vec{\mathbf{q}})\vec{\varepsilon} - \mathbf{R}(\vec{\mathbf{q}})sk(\vec{\mathbf{p}}_{tip})\vec{\alpha}$$

$$\begin{bmatrix} \vec{\alpha} \\ \vec{\varepsilon} \end{bmatrix} = \mathbf{J}_{rhs}(\vec{\mathbf{q}})\Delta\vec{\mathbf{q}}$$

$$\boxed{\delta \geq \left\| \vec{\mathbf{e}} - \left(\vec{\mathbf{d}} \bullet \vec{\mathbf{e}}\right)\vec{\mathbf{d}} \right\|}$$

Approximate this by

$$-\delta \leq \left(\vec{\mathbf{e}} - \left(\vec{\mathbf{d}} \bullet \vec{\mathbf{e}}\right)\vec{\mathbf{d}}\right) \bullet \left(Rot(\vec{\mathbf{d}}, k\pi / N)\vec{\mathbf{g}}\right) \leq \delta$$

for $0 \leq \mathrm{k} \leq N-1$

and some $\vec{\mathbf{g}}$ perpendicular to $\vec{\mathbf{d}}$

Example: Hands-on Guiding to Follow a Path

$\mathbf{F}(\vec{\mathbf{q}}) \bullet \Delta\mathbf{F}(\vec{\mathbf{q}},\Delta\vec{\mathbf{q}})$

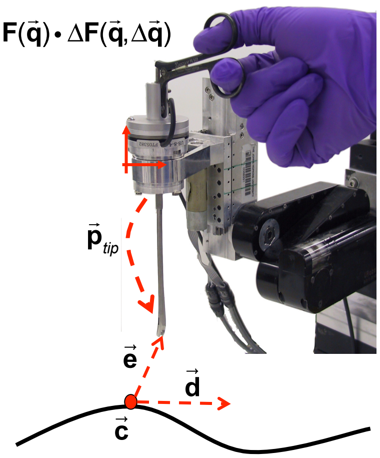

$$\Delta\vec{\mathbf{q}} = \underset{\Delta\vec{\mathbf{q}}}{\operatorname{argmin}} \left\| \mathbf{K}_v \vec{\mathbf{f}} - \mathbf{J}_{rhs}(\vec{\mathbf{q}})\Delta\vec{\mathbf{q}} \right\|^2 + \eta \left\| \vec{\mathbf{e}} - \left(\vec{\mathbf{d}} \bullet \vec{\mathbf{e}}\right)\vec{\mathbf{d}} \right\|^2$$

Such that

$$\vec{\mathbf{e}} = \vec{\mathbf{p}}(\vec{\mathbf{q}}) + \mathbf{R}(\vec{\mathbf{q}})\vec{\mathbf{p}}_{tip} + \mathbf{R}(\vec{\mathbf{q}})\vec{\varepsilon} - \mathbf{R}(\vec{\mathbf{q}})sk(\vec{\mathbf{p}}_{tip})\vec{\alpha}$$

$$\begin{bmatrix} \vec{\alpha} \\ \vec{\varepsilon} \end{bmatrix} = \mathbf{J}_{rhs}(\vec{\mathbf{q}})\Delta\vec{\mathbf{q}}$$

$$\boxed{\delta \geq \left\| \vec{\mathbf{e}} - \left(\vec{\mathbf{d}} \bullet \vec{\mathbf{e}}\right)\vec{\mathbf{d}} \right\|}$$

Approximate this by

$$-\delta \leq \left(\vec{\mathbf{e}} - \left(\vec{\mathbf{d}} \bullet \vec{\mathbf{e}}\right)\vec{\mathbf{d}}\right) \bullet \left(Rot(\vec{\mathbf{d}}, k\pi / N)\vec{\mathbf{g}}\right) \leq \delta$$

for $0 \leq \mathrm{k} \leq N-1$

and some $\vec{\mathbf{g}}$ perpendicular to $\vec{\mathbf{d}}$

Typical application domain: endoscopic sinus surgery

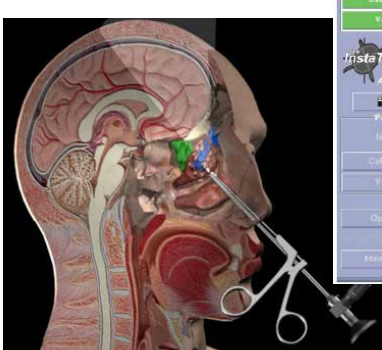

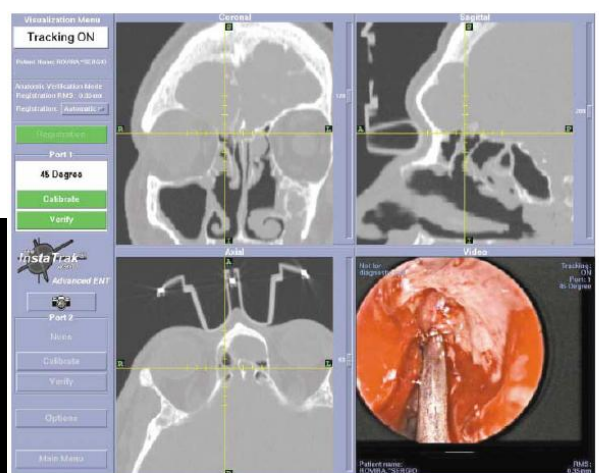

Kennedy, D.W., W.E. Bolger , S. J. Zinreich , J. Zinreich, *Diseases of the Sinuses: Diagnosis and Management*. 2001.

Sample task: steady hand path tracing

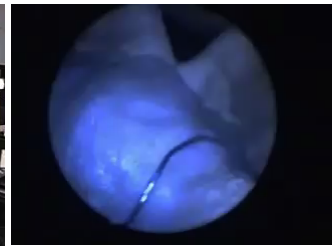

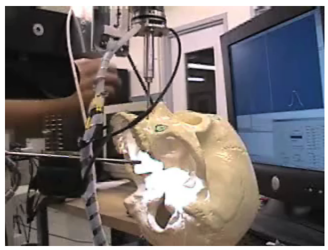

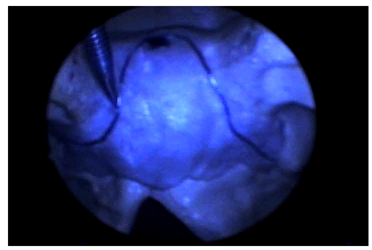

M. Li *et al.*

Goal: robotically-assisted sinus surgery

- **Difficulties with conventional approach**
  - Complicated geometry
  - Safety-critical structures
  - Limited work space
  - Awkward tools
- **Our approach**
  - Cooperatively controlled "Steady hand" robot
  - Registered to CT models
  - "Virtual fixtures" automatically derived from models

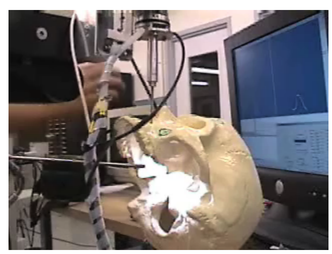

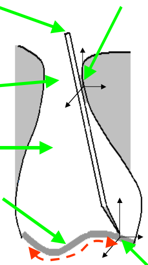

M. Li *et al.*

Experiment Setup

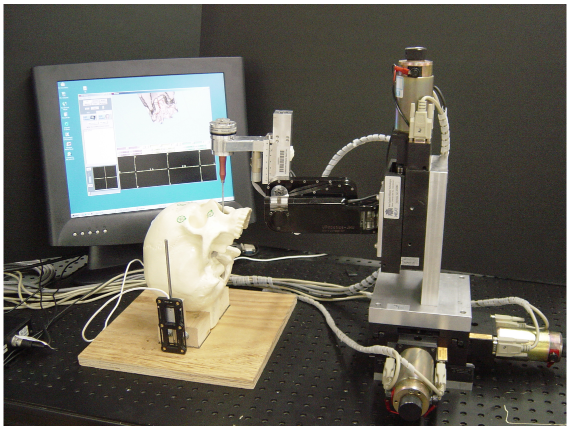

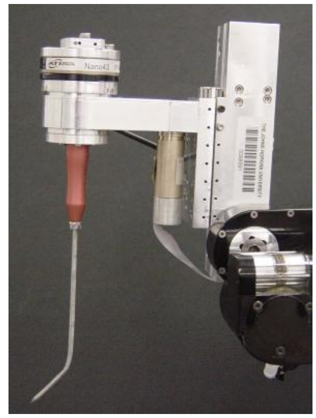

M. Li *et al.*

Experimental setup

- Plastic Skull Phantom
  - Target path defined by embedded wire
  - Radioopaque fiducials implanted on skull for registration
- Computer model
  - Extracted from CT scan using standard software (Slicer)
- 3D tracking of tools, etc. using Northern Digital Optotrak®
- Co-register model, robot, and optical tracker using standard techniques

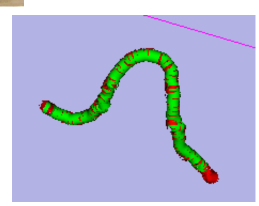

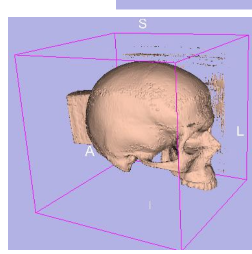

M. Li *et al.*

Virtual Fixture Online Implementation

Registered model

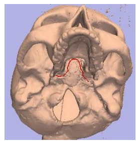

Constraint generation

Path

Tool tip guidance virtual fixture

$$\min \left\| W \cdot \left(J_{tip} \cdot \Delta q - \Delta P_{des} \right) \right\|^2$$

Subject to

$$G \cdot \Delta q \geq g$$

Robot interface

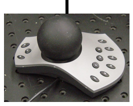

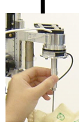

State

M. Li; R. Taylor; ICRA 2005

Boundary Constraints Generation

- Anatomy – triangulated surface models
  - Patient-specific model of nose & sinus derived from CT
  - High complexity: 182,000 triangles & 99,000 vertices
- Tool shaft -- cylinder
- The boundary constraint generation requires us to find close-point pairs between boundary surface model & tool shaft

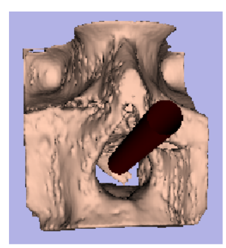

M. Li *et al.*

Boundary Constraints Generation

- Anatomy – triangulated surface models
  - Patient-specific model of nose & sinus derived from CT
  - High complexity: 182,000 triangles & 99,000 vertices
- Tool shaft -- cylinder
- The boundary constraint generation requires us to find close-point pairs between boundary surface model & tool shaft
- **Problem: How can we generate the right constraints in real time???**

M. Li *et al.*

Our solution: efficient search method using covariance tree representation of model

Covariance trees:

- Williams & Taylor, 1998; other authors
- Variation of k-d trees
- Basic idea:
  - Hierarchically split 3D model into sub-volumes
  - Realign coordinate system of each sub-volume to align with moments of inertia
- Produces bounding boxes that closely approximate boundaries & fast searches

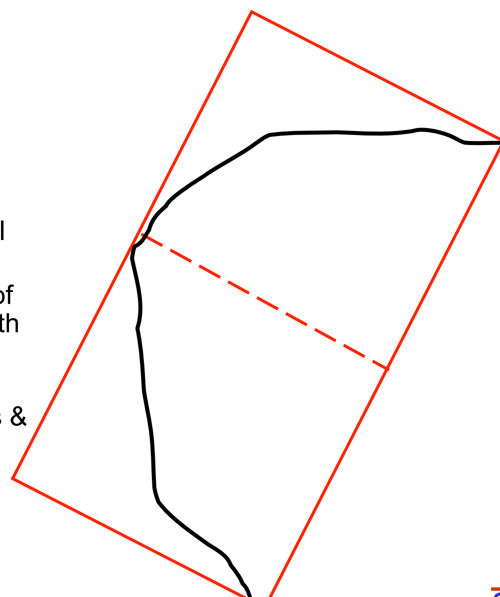

M. Li *et al.*

Our solution: efficient search method using covariance tree representation of model

Covariance trees:

- Williams & Taylor, 1998; other authors
- Variation of k-d trees
- Basic idea:
  - Hierarchically split 3D model into sub-volumes
  - Realign coordinate system of each sub-volume to align with moments of inertia
- Produces bounding boxes that closely approximate boundaries & fast searches

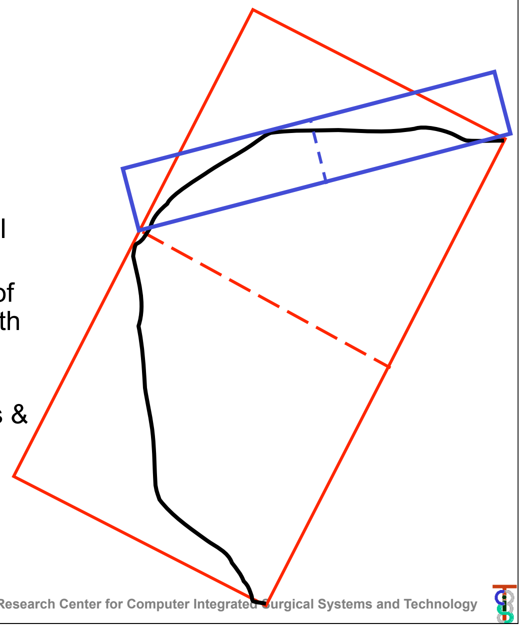

M. Li *et al.*

Our solution: efficient search method using covariance tree representation of model

Covariance trees:

- Williams & Taylor, 1998; other authors
- Variation of k-d trees
- Basic idea:
  - Hierarchically split 3D model into sub-volumes
  - Realign coordinate system of each sub-volume to align with moments of inertia
- Produces bounding boxes that closely approximate boundaries & fast searches

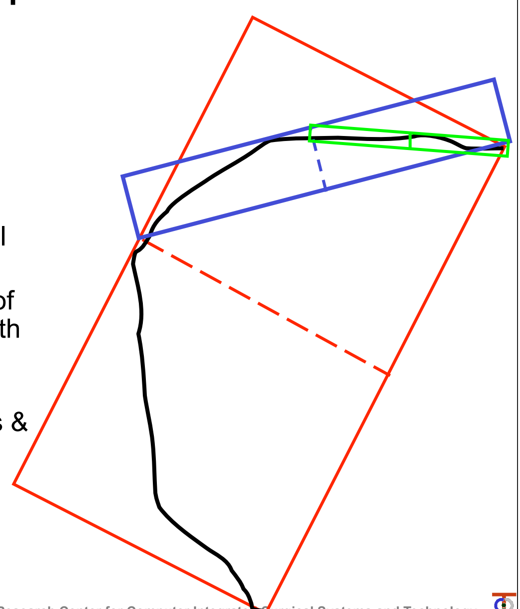

M. Li *et al.*

One difference from ICP problem

One difference from ICP problem:

- Here we in principle need to identify all anatomy that can interfere with tool shaft
- Consequently modify search to find all triangle edges that are closer than some threshold to tool shaft
- Further modify to prune search to eliminate redundant constraints
- **NOTE:** Generally, you only need to consider surfaces that are close enough so that the tool may move there in one time step.

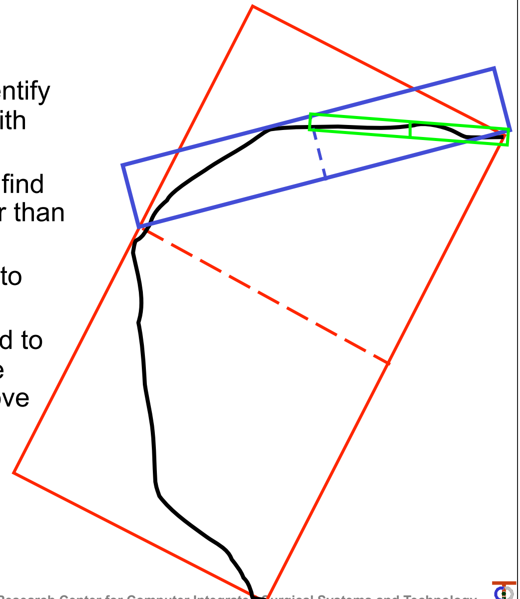

Control Implementation

- Formulate constrained least squares problem
- Constraints & objective function include terms for desired tip motion, joint limits, boundary constraints

$$\zeta = \min_{\Delta q} \left\| \begin{bmatrix} W_{tip} & & \\ & W_k & \\ & & W_{joints} \end{bmatrix} \cdot \left(\begin{bmatrix} J_{tip}(q) \\ J_k(q) \\ I \end{bmatrix} \Delta q - \begin{bmatrix} \Delta P_{tip-des} \\ 0 \\ 0 \end{bmatrix} \right) \right\|$$

$$\text{subject to} \quad \begin{bmatrix} H_{tip} & & \\ & H_k & \\ & & H_{joints} \end{bmatrix} \cdot \begin{bmatrix} J_{tip}(q) \\ J_k(q) \\ I \end{bmatrix} (\Delta q) \geq \begin{bmatrix} h_{tip} \\ h_k \\ h_{joints} \end{bmatrix}$$

M. Li *et al.*

Control Implementation

- Tip frame $\Delta P_{tip} = J_{tip}(q) \cdot \Delta q$

$\left\| \Delta P_{tip} - \Delta P_{tip-des} \right\|$ | min $\zeta_{tip} = \left\| W_{tip} \cdot \left(J_{tip}(q)\Delta q - \Delta P_{tip-des} \right) \right\|$

$\Delta P_{tip_d}{}^T \cdot \Delta P_{tip} \geq THD$ | subject to $H_{tip-des} J_{tip}(q)\Delta q \geq h_{tip}$

- Boundary constraint $\Delta P_k = J_k(q) \cdot \Delta q$

$\left\| W_k \cdot \Delta P_k \right\|$ | min $\zeta_k = \left\| W_k J_k(q)\Delta q \right\|$

$n_b^T \cdot (P_k + \Delta P_k - P_b) \geq d$ | subject to $H_k J_k(q)\Delta q \geq h_k$

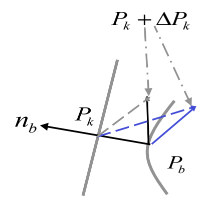

- Joints limitation

$\left\| W_{joint} \cdot \Delta q \right\|$ | min $\zeta_{joints} = \left\| W_{joints} \Delta q \right\|$

$q_{min} - q \leq \Delta q \leq q_{max} - q$ | subject to $H_{joints} \Delta q \geq h_{joints}$

M. Li *et al.*

Control implementation

- Solve problem numerically with standard methods (Lawson & Hanson, 1974)
- Performance:
  - 6 ms/iteration on 2GHz Pentium 4 PC
  - Typically 20 to 39 constraints

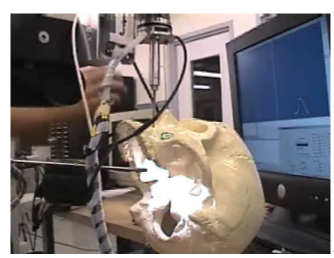

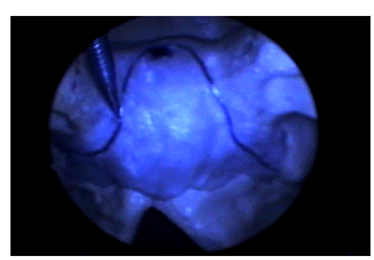

M. Li *et al.*

Results

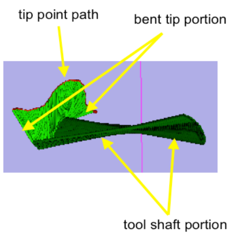

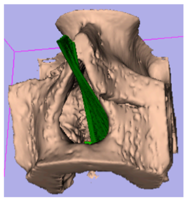

The average time in each control loop for the boundary searching is ~6ms

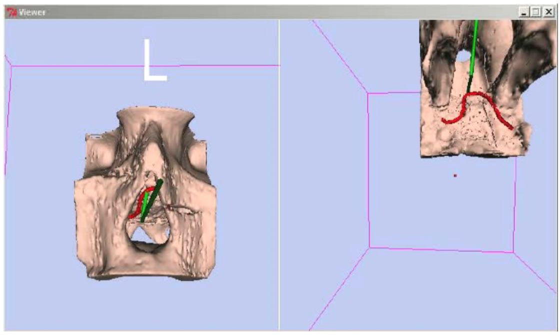

M. Li *et al.*

Results: Robot *vs* Freehand

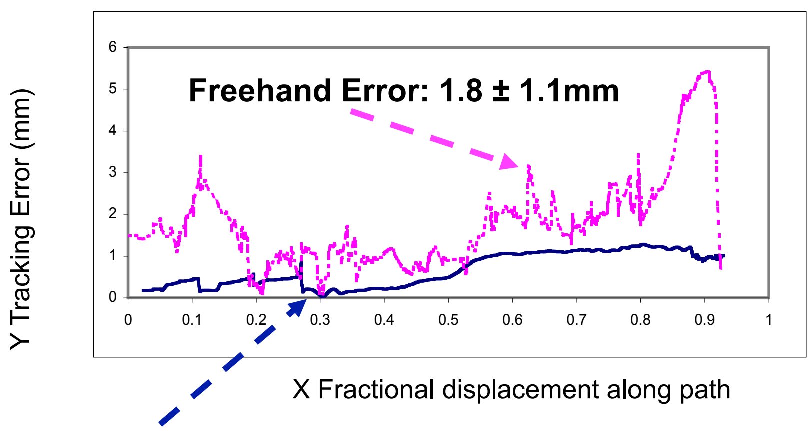

Robot Error: 0.8 ± 0.4 mm

M. Li *et al.*

Results: Robot *vs* Freehand

Trial#	Free hand		Robot Guidance	
	Average Error (mm)	Average Time (s)	Average Error (mm)	Average Time (s)
1	1.785	26.354	0.736	18.972
2	1.632	29.358	0.757	15.275
3	1.796	27.372	0.765	16.29
4	2.061	25.436	0.779	19.439
5	2.119	24.533	0.777	16.209
avg	1.819	26.611	0.763	17.237
std	1.126	1.863	0.395	1.848

Approx 1.5:1 improvement in time!

M. Li *et al.*

Combine constraints

Single Frame

Translational part

$$\begin{bmatrix} A_p \\ A_r \end{bmatrix} J(q) \cdot \Delta q \le \begin{bmatrix} b_p \\ b_r \end{bmatrix}$$

Rotational part

Multiple Frame

$$\begin{bmatrix} A_1, 0 \\ \ddots \\ 0, A_n \end{bmatrix} \begin{bmatrix} J_1(q) \\ \vdots \\ J_n(q) \end{bmatrix} \Delta q \le \begin{bmatrix} b_1 \\ \vdots \\ b_n \end{bmatrix}$$

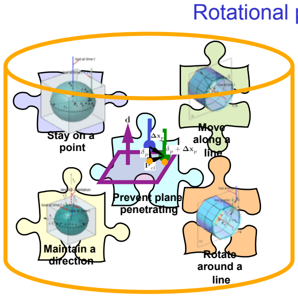

Select one or more

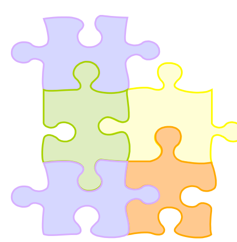

Customized virtual fixtures

M. Li, A. Kapoor

5 Basic Geometric Constraints
(Virtual fixture library)

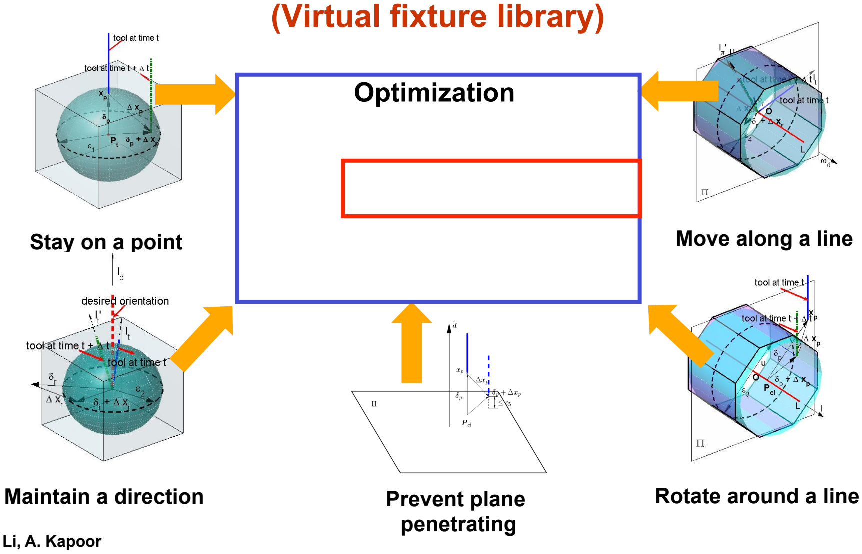

M. Li, A. Kapoor

Example: Suturing

The suturing task involves
- Select entry and exit points
- Align (Move & Orient) Needle
- Bite: Pass Needle
- Loop
- Knot

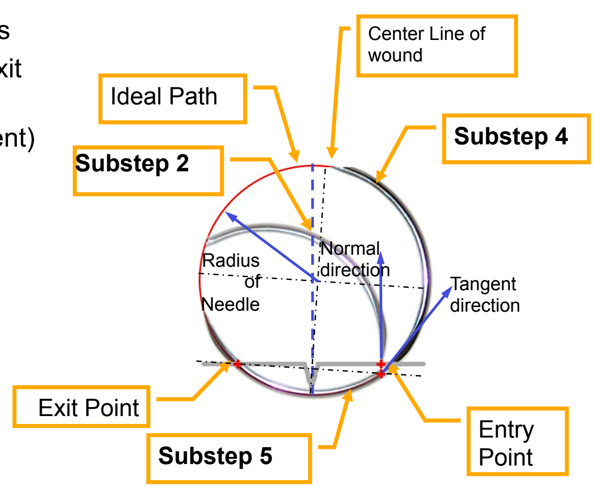

M. Li, A. Kapoor

Suturing: Align Step

0. Move Along a Line

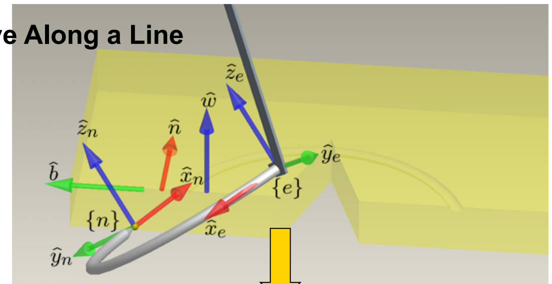

1. Stay at a point + Rotate about a line

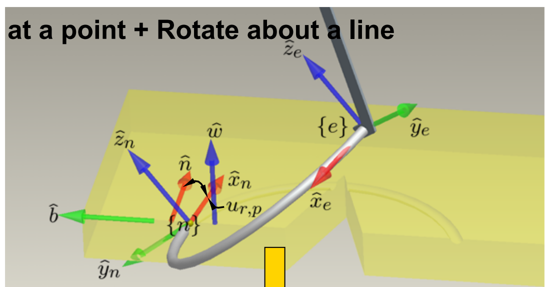

M. Li, A. Kapoor

Suturing: Align Step

2. Stay at a point + Rotate about a line

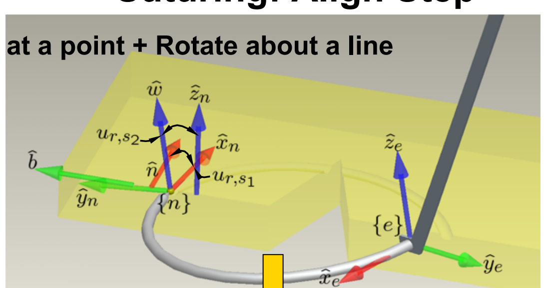

3. Puncture

4. Stay at a point + Rotate about a line

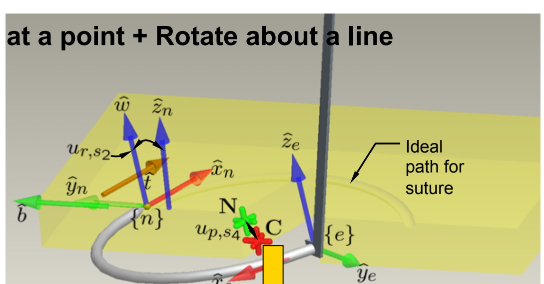

M. Li, A. Kapoor

Suturing: Bite Step

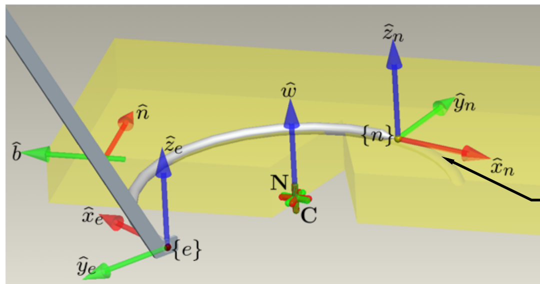

Ideal path for suture

- Ideal trajectory is a circle with radius equal to needle radius.
- Needle plane is parallel to entry and exit points and surface normal.

M. Li, A. Kapoor

Example: "Virtual fixtures" for suturing assistance

Information

Patient-specific Information (Images, lab results, genetics, etc.)

General information (anatomic atlases, statistics, rules)

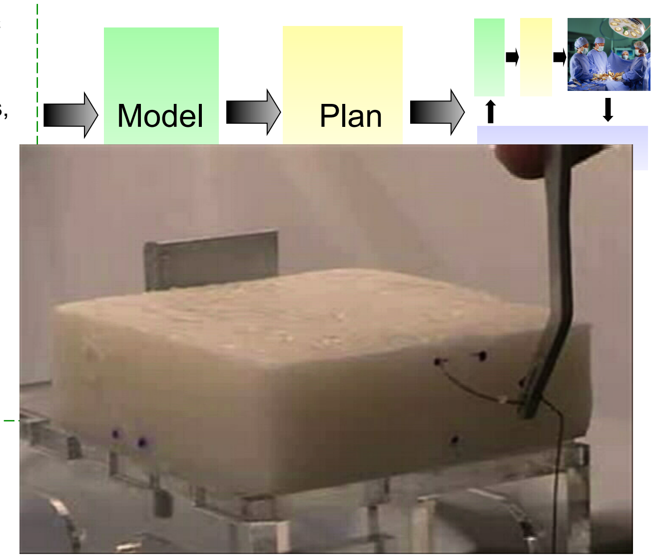

M. Li, A. Kapoor, *et al*

Suturing: Results

The average error (mm) in ideal and actual points as measured by OptoTrak®
Preliminary data collected from 4 users 5 trials each.

Error	Entry (mm)	Exit (mm)
Robot	0.6375; σ = 0.12	0.7742; σ = 0.37
Manual	--	2.1; σ = 1.2

- Suturing task using VF showed significant improvement in performance over freehand.
  - Can be performed at awkward angles
  - Avoids multiple trials and large undesirable movements inside tissue.

M. Li, A. Kapoor

Hard and soft constraints

- Constraints on the task can be “hard” or “soft”
- The relative sizes depend on the procedure, ranging from micros to tenths of millimeter.
- Soft constraints allow the controller to accommodate uncertainties inherent in surgical procedures.

Thanks: **A. Kapoor**

“Soft” constraint implementation

Suppose that we have a problem of the form

$$\Delta\vec{\mathbf{q}}_{\mathrm{des}} = \arg\min \left\| \mathrm{E}(\Delta\vec{\mathbf{q}}) \right\|^2$$

subject to a constraint of the form

$$A_i(\Delta\vec{\mathbf{q}}) \le b_i$$

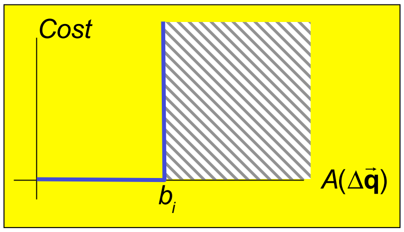

“Soft” constraint implementation

But suppose we want to make the barrier “soft”. I.e., allow the robot to go beyond the barrier at increasing cost until it hits a harder barrier later

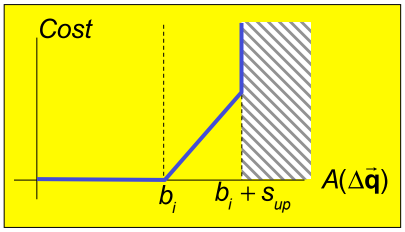

Add an explicit slack s_i and add a penalty term to the objective function

$$\Delta\vec{\mathbf{q}}_{\mathrm{des}} = \arg\min \left\| \mathrm{E}(\Delta\vec{\mathbf{q}}) \right\|^2 + \eta_i s_i^2$$

subject to a constraint of the form

$$A_i(\Delta\vec{\mathbf{q}}) - s_i \le b_i$$

$$0 \le s_i \le s_{up,i}$$

This process can be repeated several times to produce progressively steeper costs

Example: Stay near a point

Target Position: $\vec{x}_0$

After incremental motion

$\vec{x}_p + \Delta\vec{x}_p$ close to $\vec{x}_0$

We want…

$$A(\vec{x}, s) = \|\vec{\delta}_p + \Delta\vec{x}_p\|^2 - s \leq \epsilon_1$$

where $\vec{\delta}_p = \vec{x}_p - \vec{x}_0$

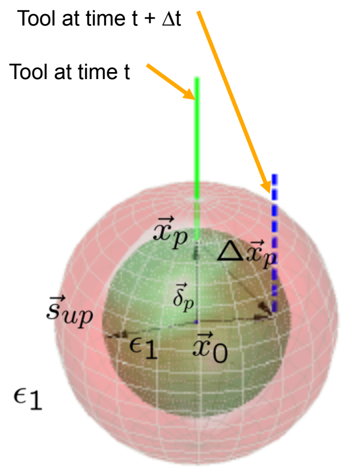

A. Kapoor, *et al.*

Using Linear Constrained Quadratic Optimization

Matrix representation

$$A \cdot \Delta\vec{x} - s \leq b$$

Use Constrained Least Squares to solve

$$\underset{\Delta\vec{q}}{\arg\min} \quad \|\Delta\vec{x} - \Delta\vec{x}^d\|^2$$

$$s.t \quad A \cdot \Delta\vec{x} - s \leq b$$

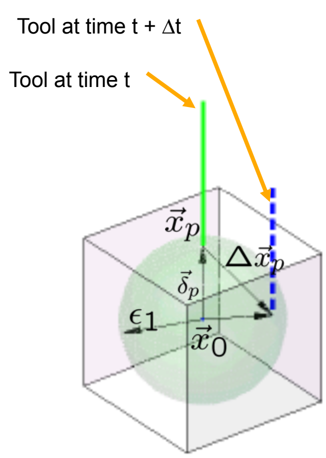

A. Kapoor, *et al.*

Linear approximation for constraints

- n x m increase
  - Polyhedron approaches the inscribed sphere
  - Linearized conditions are a better approximation
  - More constraints require more time to solve the optimization problem
- Symmetrical polyhedron
  - nxm = 4x4
- Bounded polyhedron
  - nxm = 3x3

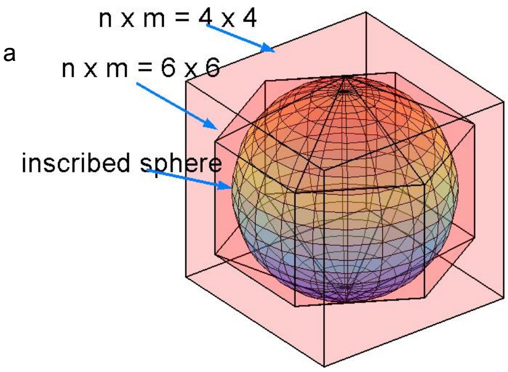

A. Kapoor, *et al.*

Example Task

- Constraint 1: Tip to move along curve C
- Constraint 2: Origin of {s} to move along
- Objective: Handle to follow user input

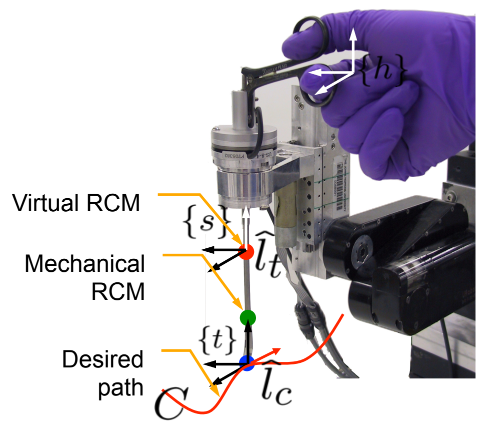

A. Kapoor, *et al.*

Results for Example Task

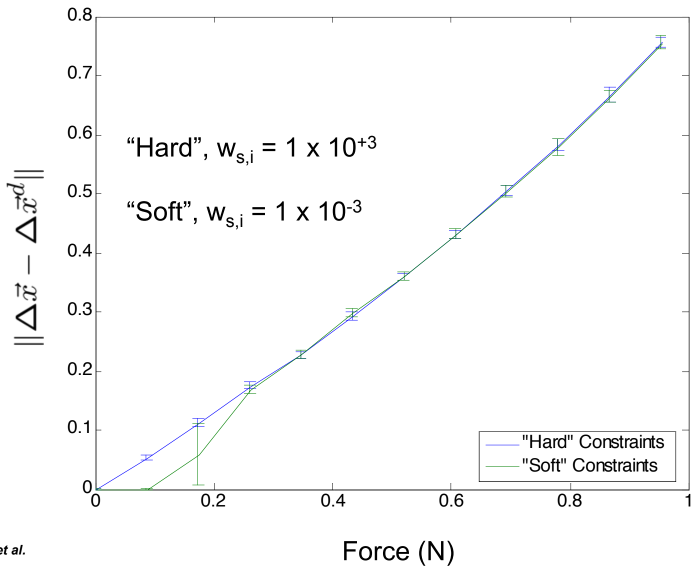

A. Kapoor, *et al.*

Nonlinear Optimization

- One problem with linearized least squares is the proliferation of constraints to approximate the real constraints
- Consequently, it is worth considering alternatives that can handle more general formulas “directly”

$$\Delta\vec{\mathbf{q}}_{des} = \arg\min_{\Delta\vec{\mathbf{q}}} C(\Delta\vec{\mathbf{x}},\Delta\vec{\mathbf{q}},\vec{\mathbf{s}})$$

subject to

$$\Delta\vec{\mathbf{x}} = \mathbf{J}\Delta\vec{\mathbf{q}}$$

$$\mathbf{A}(\Delta\vec{\mathbf{x}},\Delta\vec{\mathbf{q}},\vec{\mathbf{s}}) \le \vec{\mathbf{b}}$$

Using Non-Linear Constrained Optimization

- Use Sequential Quadratic Program* method
- SQP solves the following problem iteratively

$$\mathbf{d}^{(k)} = \arg\min_{\mathbf{d}^{(k)}} \quad \nabla C\big(\mathbf{x}(\mathbf{q}+\Delta\mathbf{q}^{(k)}), \mathbf{s}^{(k)}, \mathbf{x}^{d}\big)^{T}\mathbf{d}^{(k)} + \frac{1}{2}\mathbf{d}^{(k)T}\mathbf{B}^{(k)}\mathbf{d}^{(k)}$$

$$\text{s.t.} \quad \nabla A_j\big(\mathbf{x}(\mathbf{q}+\Delta\mathbf{q}^{(k)}), \mathbf{s}^{(k)}\big)^{T}\mathbf{d}^{(k)} \le b_j; \quad j \in \mathcal{A}_k$$

- Start with a solution $[\Delta q^k, s^k]^t$
- Descent direction along with step size determine next solution $[\Delta q^{k+1}, s^{k+1}]^t$

*P. Spellucci, *Math. Prog.*, '98

A. Kapoor, *et al.*

Remarks: Non-Linear Constraints

- Current incremental motion can be used as starting guess for next motion
- Worst case number of constraints n times m, n = # variables, m = # nonlinear constraints
- Analytical gradient increases speed

A. Kapoor, *et al.*

Linear v. Non-Linear Constraints

Accuracy

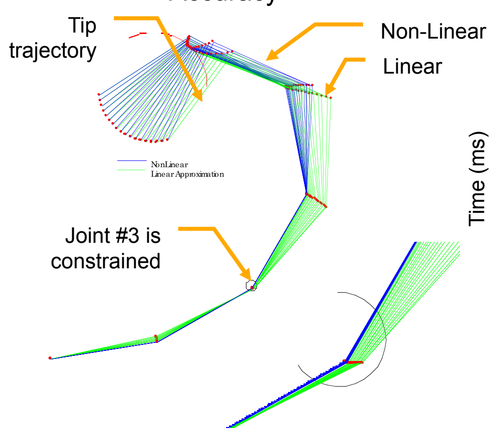

Time

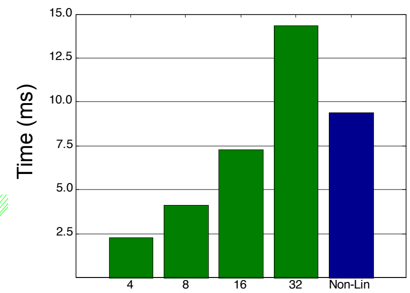

Hyperplanes used for approximation

A. Kapoor, *et al.*

Effect of increasing control-loop time

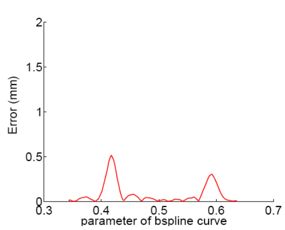

Interval: 150ms

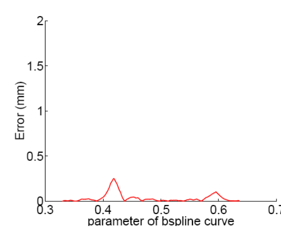

Interval: 40ms

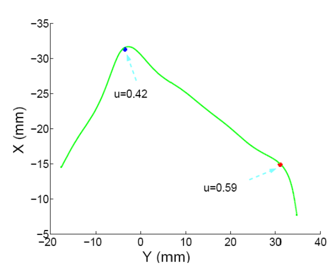

- Large error at sharp turning
- Small interval reduces error

Ming Li et al., IROS '05

Example: Two-handed virtual fixture for centering knot with visual feedback

Information

Patient-specific Information (Images, lab results, genetics, etc.)

General information (anatomic atlases, statistics, rules)

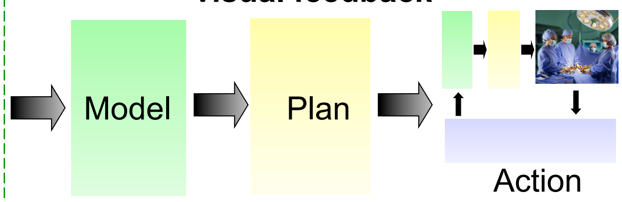

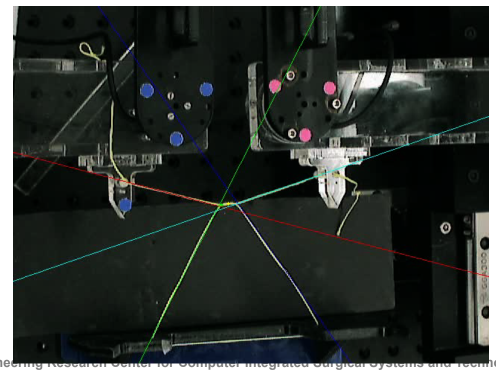

Ankur Kapoor

High Dexterity in a Small Package

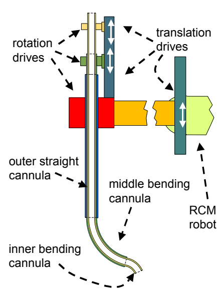

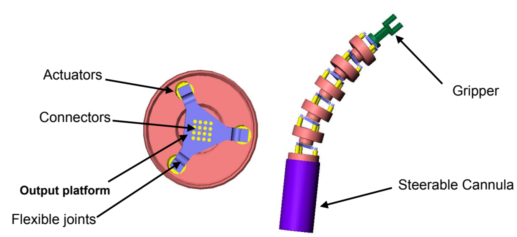

Taylor, Shoham, *et al.* 2002

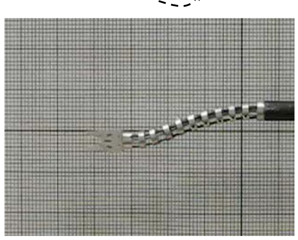

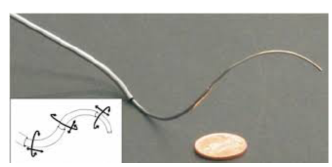

Webster *et al., 2006*

Simaan, Taylor *et al.* 2004, 2007

Scalable Robot for Dexterous Surgery in Small Spaces (aka Snake Like Robot)

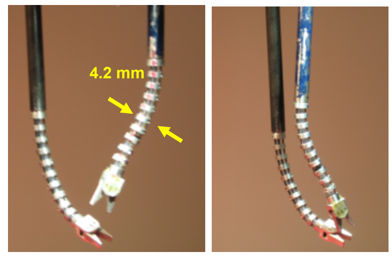

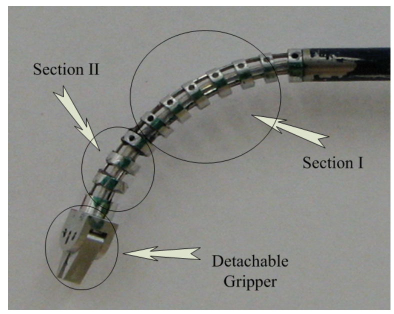

P. Kazanzides, R. H. Taylor
Collaborator: P. Flint, MD

Snake Like Robot
System Architecture

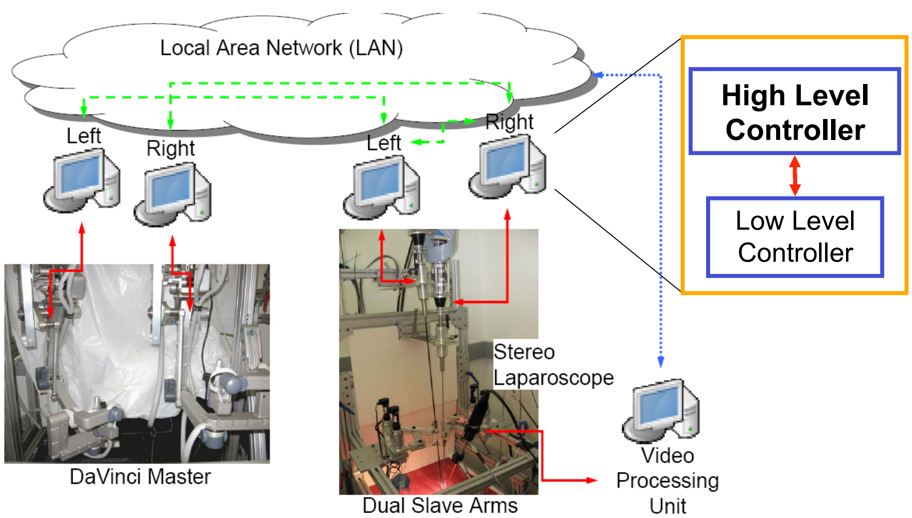

DaVinci Master Robot

High Level Constrained Control

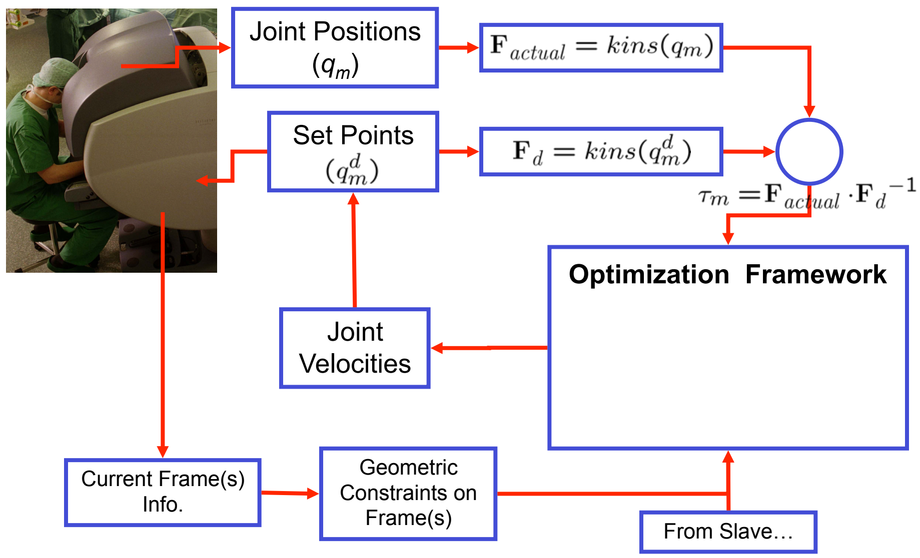

Master Side High-Level Controller

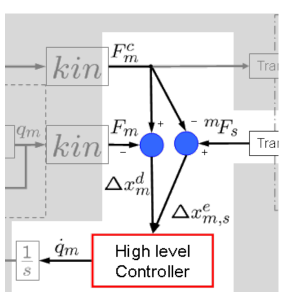

$$\min_{\Delta\vec{q}_m} \left\| W_{m,t}\left(\Delta x_m - K_a\left[p_m^e; \theta_m \omega_m\right]\right)\right\|$$

$$+ \left\| W_{m,s}\left(\Delta x_m - K_f\left[p_{m,s}^e; \theta_{m,s}\omega_{m,s}\right]\right)\right\|$$

$$+ \left\| W_{m,j} \Delta q_m \right\|$$

- **Objectives**:
  - Minimize error between desired motion and actual motion
  - Oppose motion that increases master-slave tracking error
  - Minimize the extraneous motion of the joints, and
  - Avoid large incremental joint motions that could occur near singularities

Master Side High-Level Controller

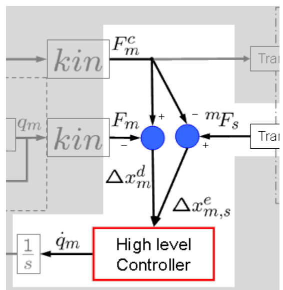

$$H_m \Delta q_m \geq h_m$$

that is $\begin{bmatrix} I \\ -I \\ I \\ -I \end{bmatrix} \Delta q_m \geq \begin{bmatrix} q_{m,L} - q_m \\ q_m - q_{m,U} \\ \dot{q}_{m,U} \cdot \Delta t \\ \dot{q}_{m,U} \cdot \Delta t \end{bmatrix}$

- **Constraints**:
  - General form: $H_{m,j} + \Delta q_m \geq h_{m,j}$
  - Not allow motion outside joint range
  - Not allow motion that exceeds joint velocity limits
  - Additional constraints can be added from the VF Library

DaVinci Slave Robot
High Level Constrained Control

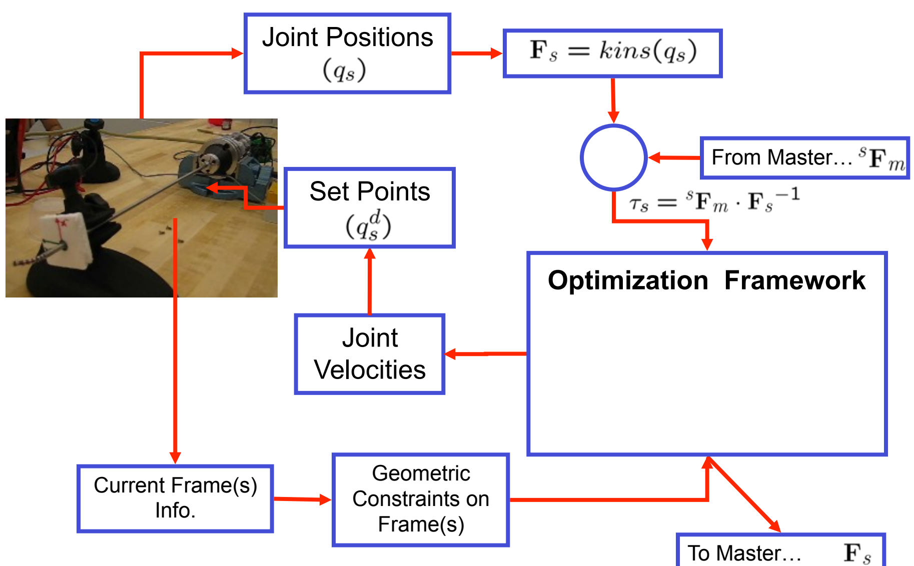

Slave-Side Snakes

- Actual snake section bends are a fairly complicated function of the linear displacements of the individual tubes and wires in the bending parts. But these displacements can be computed from the desired bending angles.
- Therefore, create pseudo-"joints" q_{sec1} and q_{sec2} corresponding to the bending angles in the two bend sections.
- Solve the optimization problem for q_{sec1} and q_{sec2} and the other joint angles of the slave robot. Then compute linear displacements from q_{sec1} and q_{sec2}. This also involves some calculations for redundancy resolution that can be done with a similar optimization method or can be done analytically.



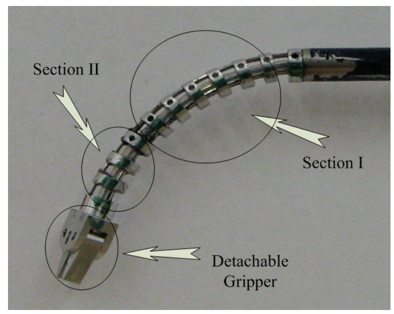

Slave Side High-Level Controller

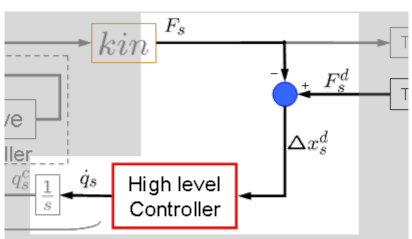

$$\min_{\Delta \vec{q}_s} \left\| W_{s,t} \left(\Delta x_s - K_a \left[p_s^e ; \theta_s \omega_s \right] \right) \right\| + \left\| W_{s,j}(q) \Delta q_s \right\| + \left\| W_{s,s} s \right\|$$

- **Objectives**:
  - Minimize error between desired motion and actual motion
  - Minimize the extraneous motion of the joints, and
  - Avoid large incremental joint motions that could occur near singularities

Slave Side High-Level Controller

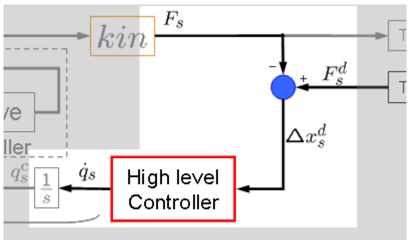

such that $\begin{bmatrix} I \\ -I \\ I \\ -I \end{bmatrix} \Delta q_s \geq \begin{bmatrix} q_{s,L} - q_s \\ q_s - q_{s,U} \\ \dot{q}_{s,U} \cdot \Delta t \\ \dot{q}_{s,U} \cdot \Delta t \end{bmatrix}$

and $\|\vec{d}\| + \Delta x_b \cdot \hat{d}$
$+ \vec{v} \cdot \hat{d} + s \geq d_{safe}$
$0 \leq s \leq s_{lim}$

- **Constraints**:
  - Not allow motion outside joint range
  - Not allow motion that exceeds joint velocity limits
  - **Collision avoidance between slaves**
  - More constraints can be added from the VF Library

Single Port Access Surgery

Nabil Simaan (Vanderbilt, Columbia), with P. Allen (Columbia), D. Fowler (Columbia)

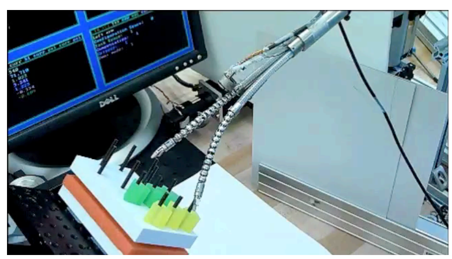

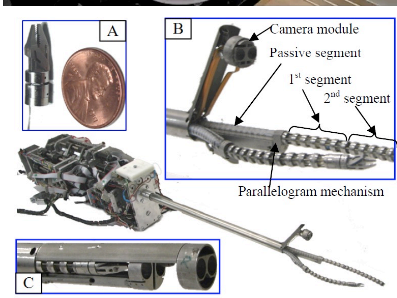

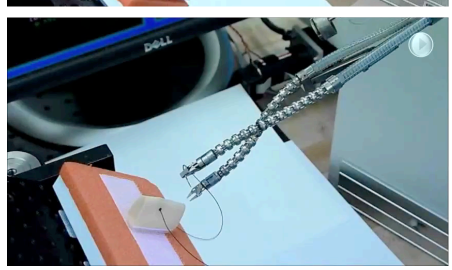

New technology finally allows true evaluation of the potential of single port access surgery. Systems raise new questions about control and telemanipulation infrastructure/cooperative control.

Single Port Access Robotic Surgery

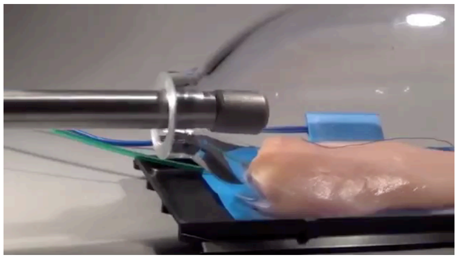

Titan Medical Sport
https://www.youtube.com/watch?v=jIvjvcKA6xQ

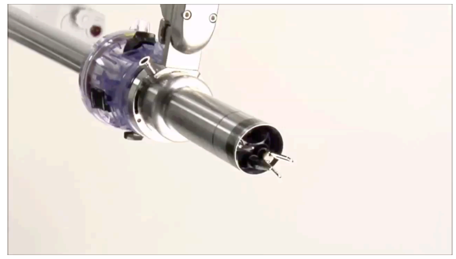

Intuitive Surgical Sp
https://www.youtube.com/watch?v=-jm63JdTrp4

Robot-Assisted Skull Base Surgery

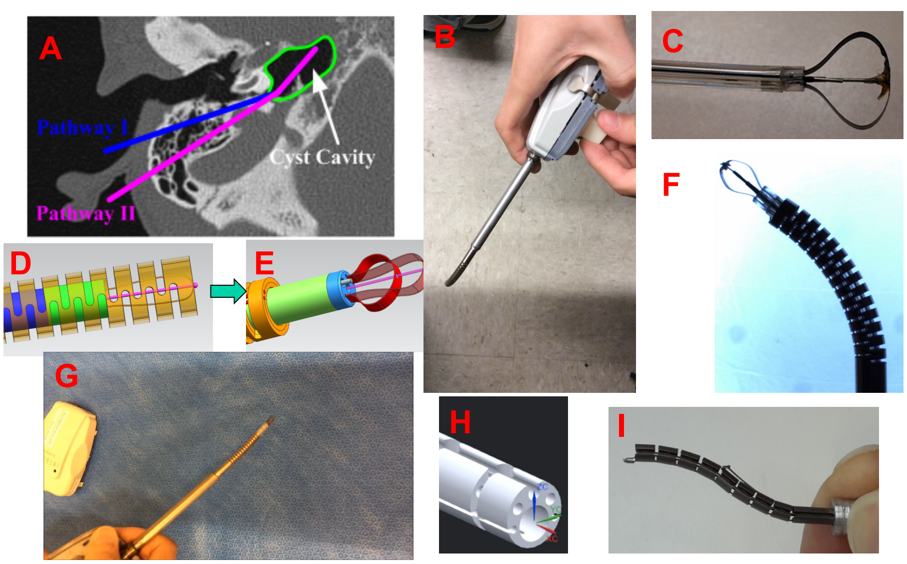

Integration of a Snake-like Dexterous Manipulator for Head and Neck Surgery with the da Vinci Research Kit

S. Coemert, F. Alambeigi, A. Deguet, J. P. Carey, M. Armand, T. C. Lueth, R. H. Taylor

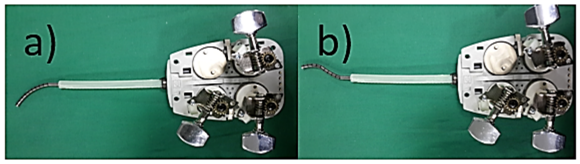

Handheld actuation concept: a) C-shaped b) S-shaped

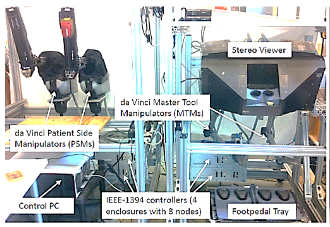

Overview of the DVRK system [5]

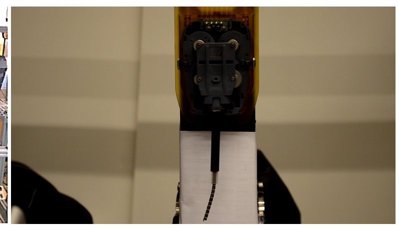

Video: Actuation of the SDM attached to DVRK

S. Coemert, F. Alambeigi, A. Deguet, J. P. Carey, M. Armand, T. C. Lueth, and R. H. Taylor, "Integration of a Snake-like Dexterous Manipulator for Head and Neck Surgery with the da Vinci Research Kit", in *Hamlyn Symposium on Medical Robotics*, London, June 26-27, 2016. pp. 58-59.

APL Large Lumen, Dexterous Snake for MIS

- Joint project with JHU APL
- Innovative fabrication process completely isolates drive cables
- Current prototypes
  - 2 DoF (C-bend) and 4DoF (S-bend)
  - Nitinol structure with high stiffness
  - 6 mm OD; Large 4 mm lumen allows insertion of surgical instruments
- Initial application: Minimally-invasive curettage of osteolytic lesions

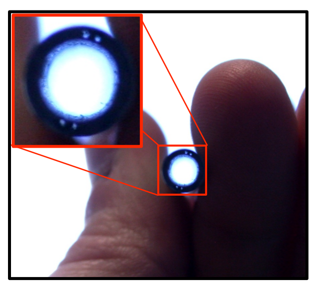

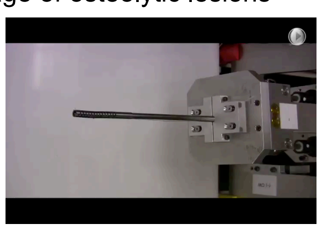

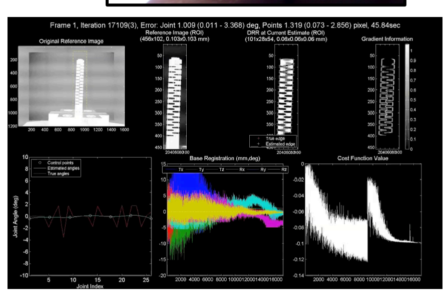

M. Armand, R. Taylor, M. Kutzer, R. Murphy, S. Segrett,i F. Alambeigi, I. Iordachita, H. Liu, Y. Otake *et al.*

Treatment of Osteolytic Lesions

- Indication: Osteolysis behind a well-fixed acetabular component
  - Leads to component loosening and failure of THA
- Surgical Goals
  - Minimally invasive removal of the osteolytic lesion
  - Treatment of the lysis without full replacement of the acetabular component
- Surgical Procedure
  - Access the lesion through the screw holes of the acetabular component (minimally invasive)
  - Remove and grafting the lesion
  - Replace the polyethylene liner

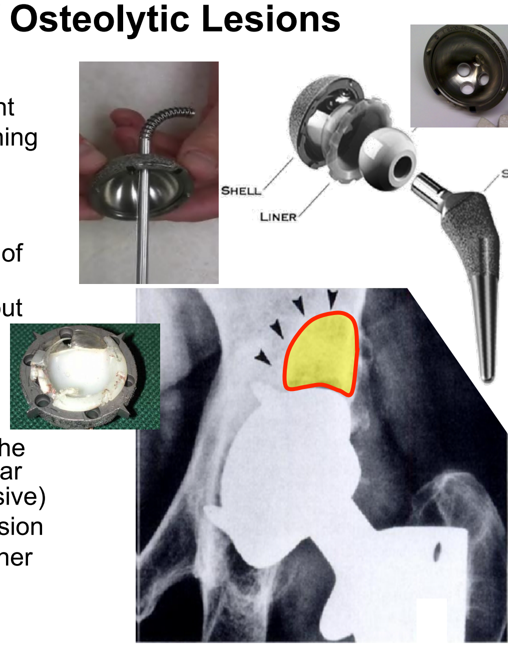

Minimally-Invasive Osteolysis Curettage

M. Armand, R. Taylor, M. Kutzer, R. Murphy, S. Segrett,i F. Alambeigi, I. Iordachita, H. Liu, Y. Otake P. Wilkening, *et al.*

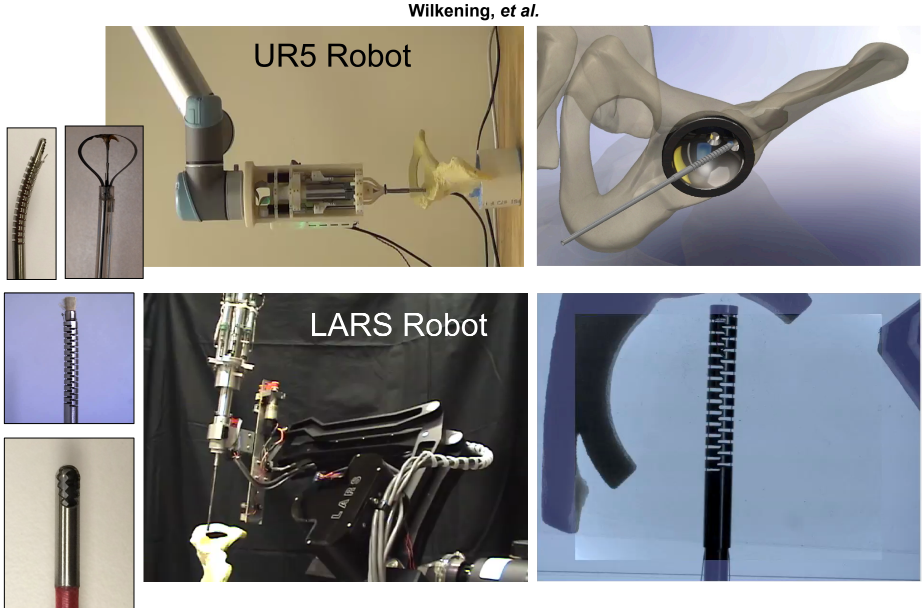

Novel Shape Sensor Array (SSA) for Large Curvature Detecting

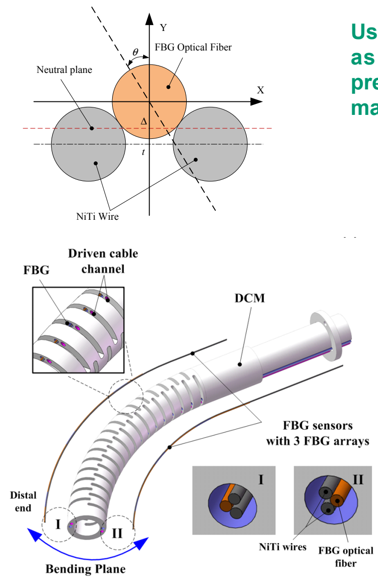

Using FBG sensors along with nitinol wires as the supporting substrates, we can prevent local stress concentration, therefore maximizing curvature detection range.

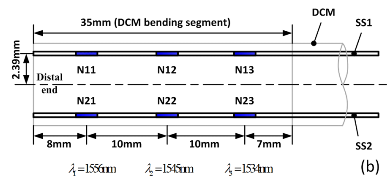

(b)

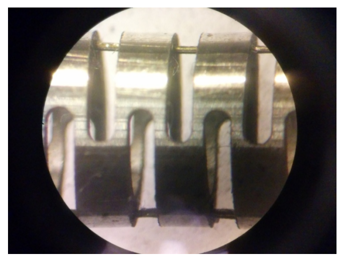

Hao Liu, Amirhossein Farvardin, Sahba Aghajani Pedram, Iulian Iordachita, Russell H. Taylor, Mehran Armand

Novel Shape Sensor Array (SSA) for Large Curvature Detecting

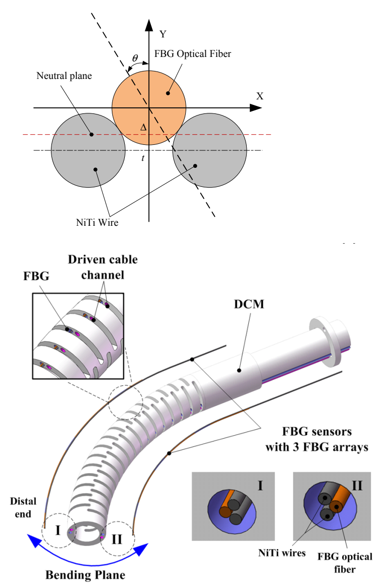

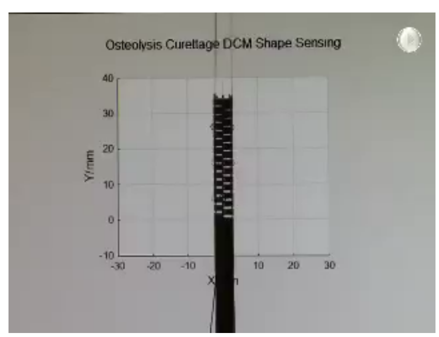

Hao Liu, Amirhossein Farvardin, Sahba Aghajani Pedram, Iulian Iordachita, Russell H. Taylor, Mehran Armand

Curved Drilling of the Femoral Head

Alambeigi, *et al.*

- Osteonecrosis of the femoral head
  - More than 20,000 patients per year
  - To reduce the pressure in the femoral head, core decompression was developed more than three decades ago.
- Steerable "snake" with flexible drill provides better

Farshid Alambeigi, Yu Wang, Shahriar Sefati, Ryan. J. Murphy, Iulian Iordachita, Russell H. Taylor, Harpal Khanuja, and Mehran Armand, "Curved-Drilling Approach in Core Decompression of the Femoral Head Osteonecrosis Using a Continuum Manipulator", *Proc. ICRA 2017*

Curved Drilling of the Femoral Head

Alambeigi, *et al.*

- Sample Holder Mechanism: feeding motion and 6DOF force se
- Thermal Camera: "Real-time" tracking of the cutter

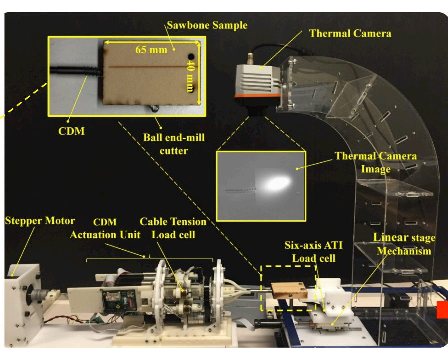

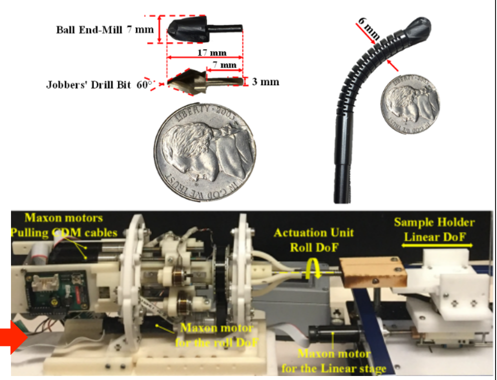

Farshid Alambeigi, Yu Wang, Shahriar Sefati, Ryan. J. Murphy, Iulian Iordachita, Russell H. Taylor, Harpal Khanuja, and Mehran Armand, "Curved-Drilling Approach in Core Decompression of the Femoral Head Osteonecrosis Using a Continuum Manipulator", *Proc. ICRA 2017*

Curved Drilling of the Femoral Head

Alambeigi, *et al.*

S-Shape and multiple branch curved-drilling

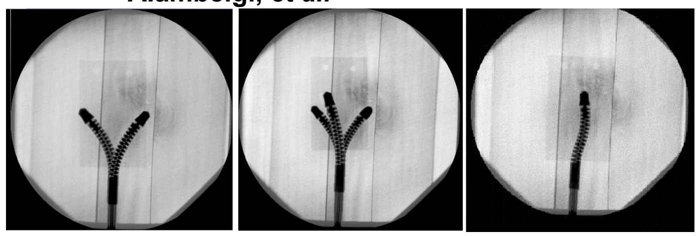

Curved-Drilling Experiments on human cadaver specimens

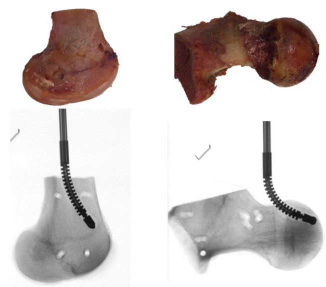

Farshid Alambeigi, Yu Wang, Shahriar Sefati, Ryan. J. Murphy, Iulian Iordachita, Russell H. Taylor, Harpal Khanuja, and Mehran Armand, "Curved-Drilling Approach in Core Decompression of the Femoral Head Osteonecrosis Using a Continuum Manipulator", *Proc. ICRA 2017*

Challenges in Precise Minimally Invasive Head-and Neck Surgery

- Long (25cm) instruments
  - amplify hand tremor
  - reduce precision
- Tight spaces near sensitive anatomy
- Limited working area

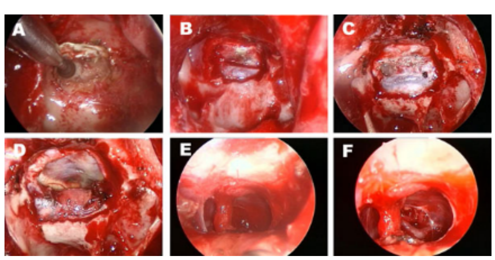

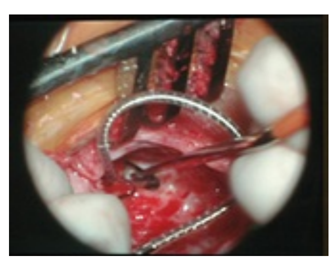

The Robotic ENT Microsurgery System (REMS)

User interface:
- Hands-on control, surgeon "in the game"
- Foot pedal-controlled gain

Technical specs:
- Up to 0.025 mm precision on-demand
- 6 degrees of freedom
- 125x125x125mm work volume
- Calibrated accuracy ~50-150µm

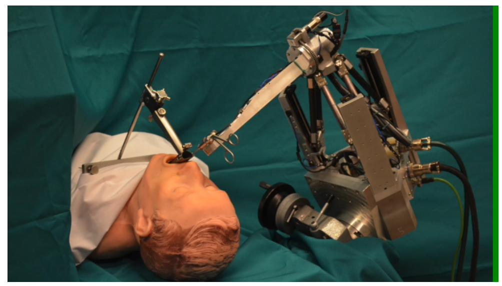

Control modes:
- Free hand
- Remote center of motion
- Virtual fixture avoidance
- Teleoperation

K. Olds, *Robotic Assistant Systems for Otolaryngology-Head and Neck Surgery,* PhD thesis in Biomedical Engineering, Johns Hopkins University, Baltimore, March 2015.

Playing the "Operation Game" with Long Instruments

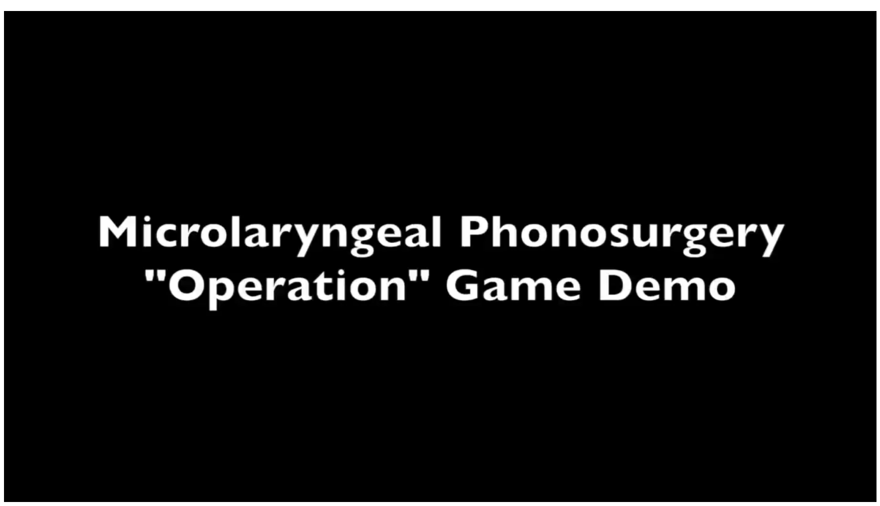

K. Olds, *Robotic Assistant Systems for Otolaryngology-Head and Neck Surgery,* PhD thesis in Biomedical Engineering, Johns Hopkins University, Baltimore, March 2015.

REMS Typical Applications

Laryngeal / Vocal Cord

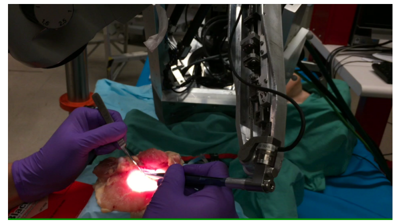

Open Microsurgery

Image-guided sinus surgery with virtual fixtures

Other applications include:

- Otology
  - Stapes surgery
  - Mastoidectomy
  - Cochlear implant
- Craniotomy
- Spine
- Hand
- …

Vitreoretinal Microsurgery

British Journal of Ophthalmology 2004 - Akifumi Ueno et al

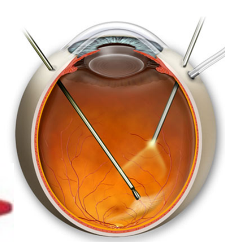

www.eyemdlink.com

Alcon Vitreosurgery Instrument

Microsurgery Assistant Workstation

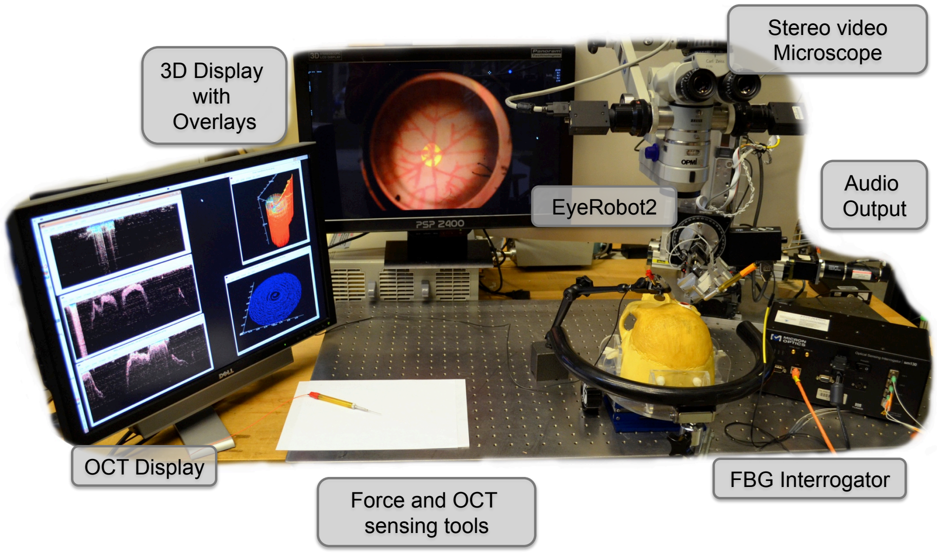

Retina Mosaicking, Annotation, and Registration

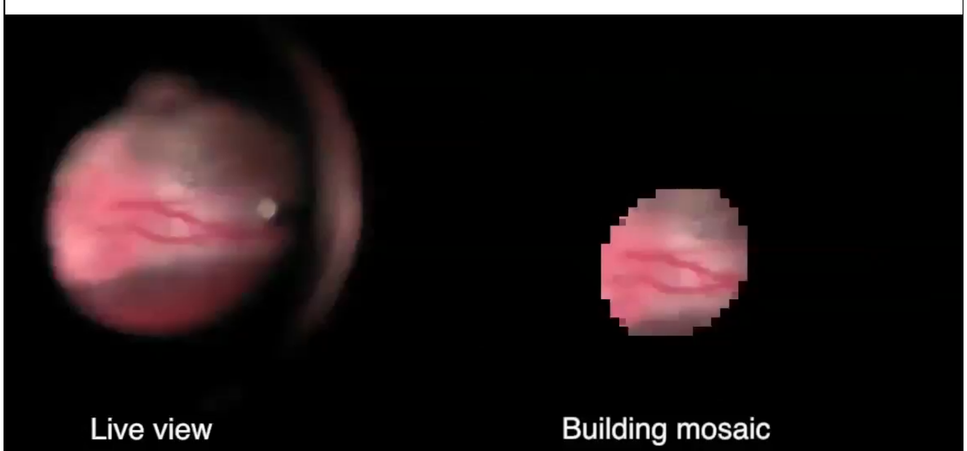

R. Richa, B. Vagvolgyi, R. Taylor, G. Hager, *MICCAI 2012*,

JHU Steady Hand "Eye Robot"

Russell Taylor, Iulian Iordachita, D. Gierlach, D. Roppenocker, *et al.*

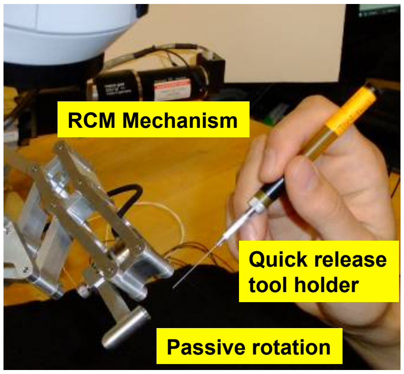

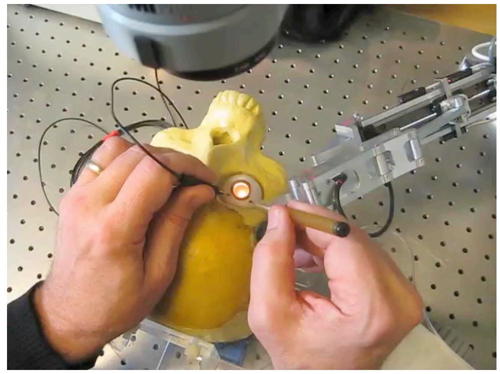

- Highly precise robot
- Hands-on cooperative control or teleoperation
- Several generations in lab
- Precise, stable platform for developing "smart" surgical instruments and sensors
- Virtual fixtures and advanced control

Retinal Microsurgery – *in vivo* experiments

- Overall System Performance
- System Ergonomics
- Collect Data
  - Robot / Force / OCT
  - Video / Audio

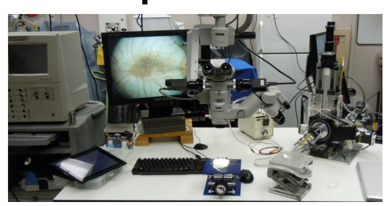

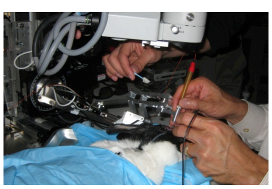

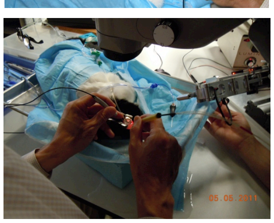

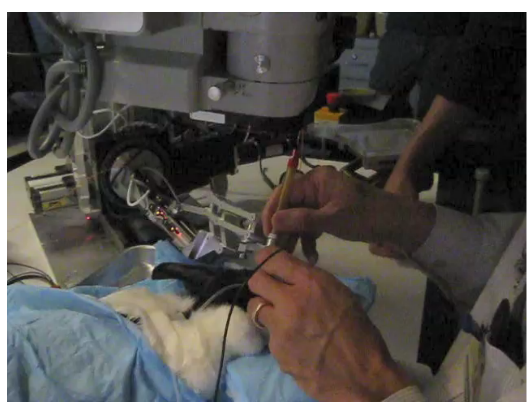

Force-Sensing Micro-Forceps Tools for Vitreoretinal Surgery

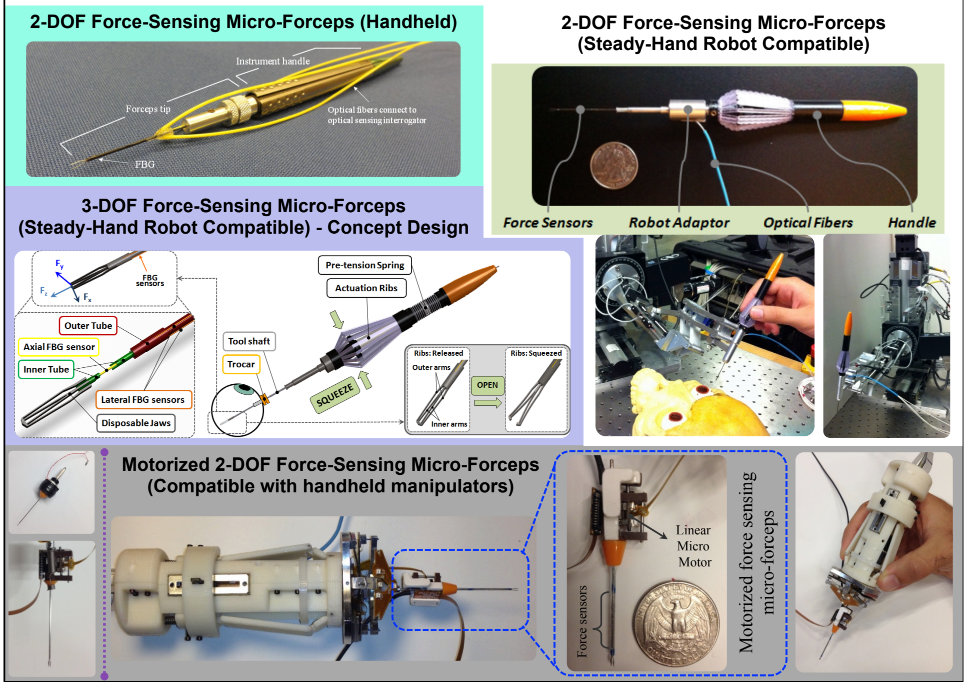

In-vivo experiments

- Test the force sensing micro-forceps in-vivo using rabbit in the operating room
- Force measurements, stereo microscopic video, and surgeon’s voice annotation were recorded with timestamps for synchronization and analysis

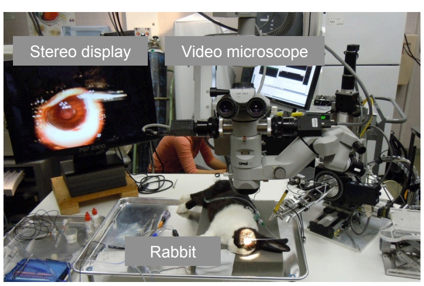

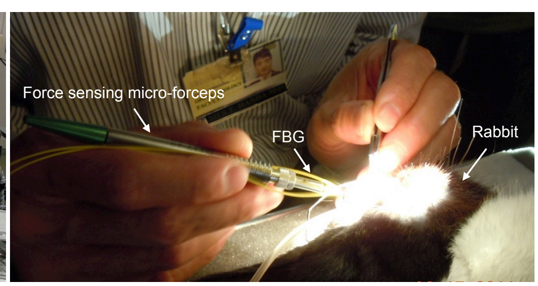

Xingchi He, Marcin Balicki, Jin U. Kang, Peter Gehlbach, James Handa, Russell Taylor, Iulian Iordachita
“Force sensing micro-forceps with integrated fiber Bragg grating for vitreoretinal surgery”, SPIE 202

Video overlay of tool tip forces

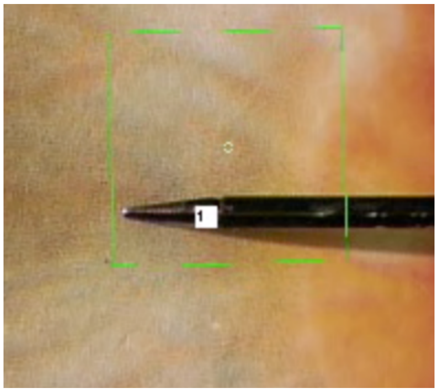

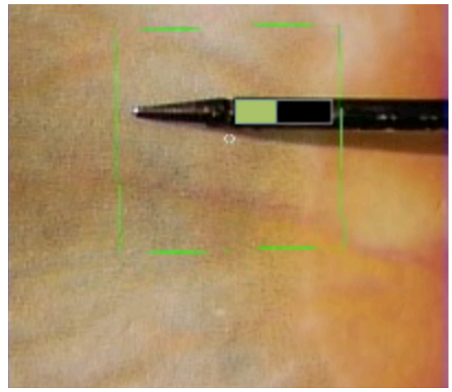

Use of Audio and Voice

- Voice commands and annotation
- Auditory sensory substitution

Example Audio Response to Force Input

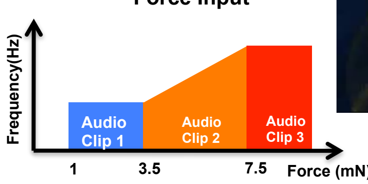

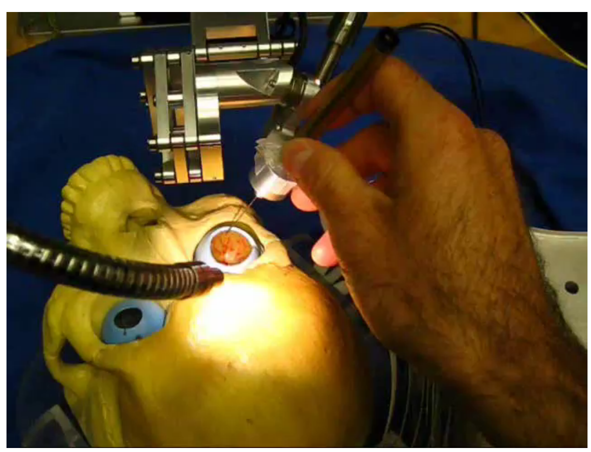

M. Balicki, *et al.*

Dual Force Sensor

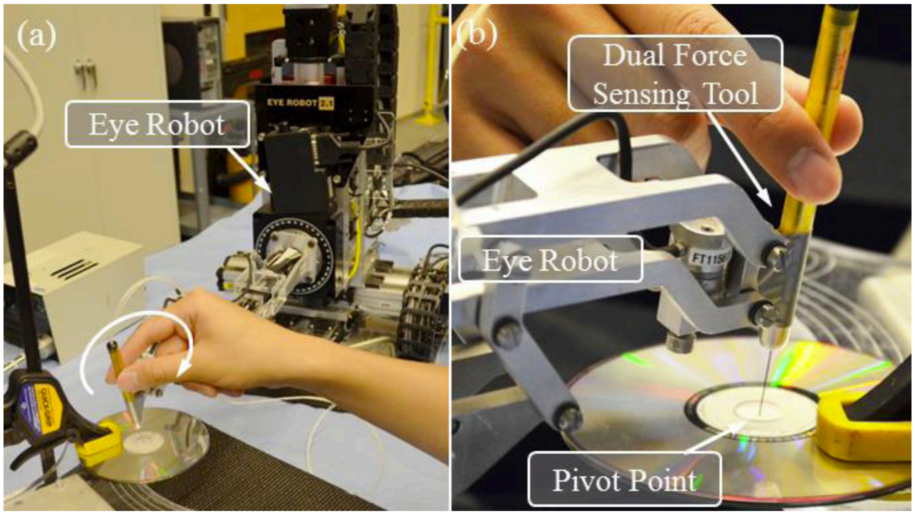

X. He, Marcin Balicki, P. Gehlbach, J. Handa, R. Taylo, and I. Iordachita, "Variable Admittance Robot Control with A New Dual Force Sensing Instrument for Retinal Microsurgery", *in IEEE Int. Conf. Rob. Automat*, Hong Kong, May 31-June 5, 2014..

Dual Force Sensor

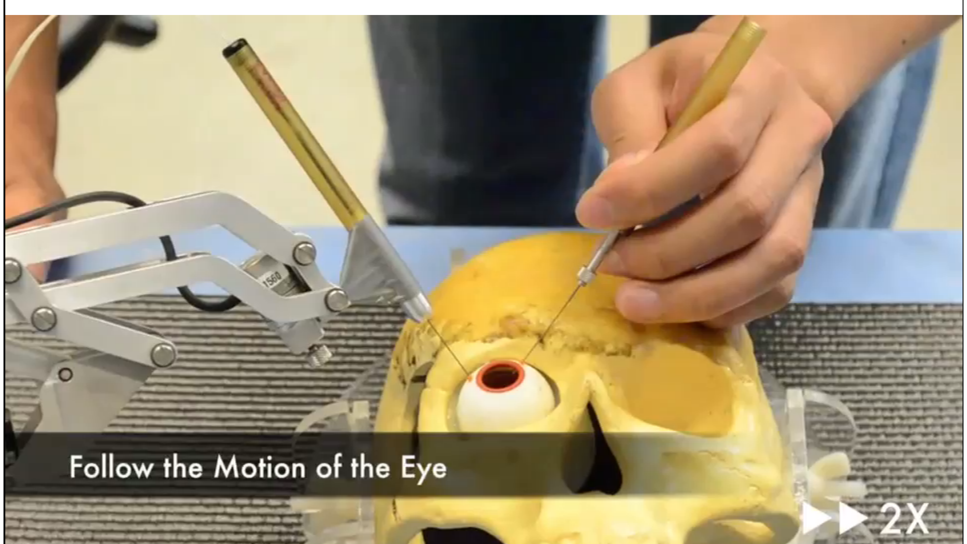

X. He, Marcin Balicki, P. Gehlbach, J. Handa, R. Taylo, and I. Iordachita, "Variable Admittance Robot Control with A New Dual Force Sensing Instrument for Retinal Microsurgery", *in IEEE Int. Conf. Rob. Automat*, Hong Kong, May 31-June 5, 2014..

µForce Scaling Cooperative Control

Cooperative Control

Velocity at the tool (V) is proportional to (α gain) the user's input force at the handle (F_h)

$$\dot{x} = \alpha F_h$$

µForce Scaling

Amplifies (ϒ gain) the human-imperceptible forces sensed at the tool tip (F_t) to handle interaction forces (F_h) by modulating robot velocity.

$$\dot{x} = \alpha \left(F_h - \gamma F_t \right), \quad \text{e.g., } \gamma = 500$$

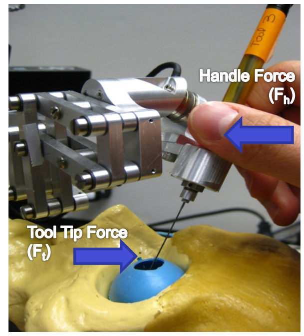

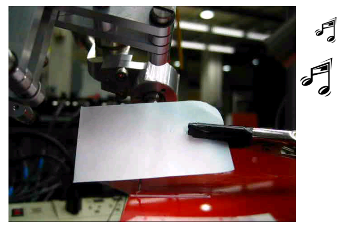

Kumar et al (ICRA' 00) ; Balicki et al. (MICCAI'10); Uneri et al., BioRob 2010

µForce Guided Cooperative Control

- ¬ User fights against ever increasing resistance
- ✓ Ensure safety tip force limits
- ¬ User interaction is limited at high-resistance regions
- ✓ Try to avoid those regions for later peeling
- ¬ User gets "stuck", gives up, tries re-approach
- ✓ Ensure continuous user motion, even at the boundaries

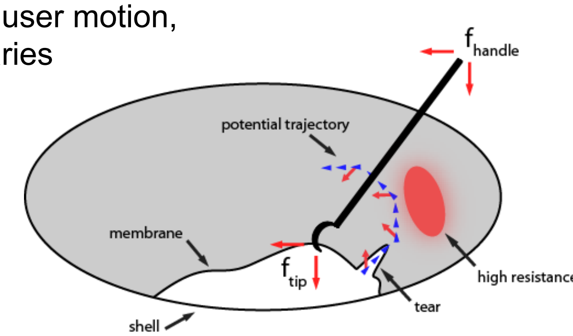

Uneri *et al.*, BioRob 2010

μForce Guided Cooperative Control

- Global Limiting
  - Task-specific tip force limit
  - User controlled limit distribution
- Continuous motion at the constraint boundaries
- Virtual spring construct to ensure stability

$$f_{lim} = f_{max} \frac{|f_h|}{\|f_h\|}$$

$$\dot{x}_{lim} = \dot{x} \left(\frac{f_{lim} - |f_t|}{f_{spring}} \right)$$

Local Force Minimization

•Guiding user towards direction of minimum resistance

•Sensitivity variable allows user override

•Haptically intuitive response

•Avoids / postpones reaching limits

$$\dot{x}_{min} = k_p \left(1 - s \frac{|f_t|}{\|f_t\|} \right) f_h$$

Uneri *et al.*, BioRob 2010

Experimental Platform

Focusing on:

•Properties of the tissue we interact with

•The method of interaction, i.e. performance of our algorithms

Performed on:

- **Inner shell membrane of raw eggs**
- **Surrogate tissue for epiretinal membrane peeling**

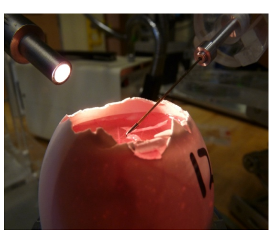

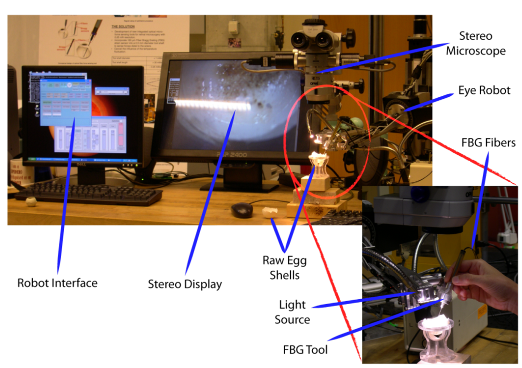

Uneri *et al.*, BioRob 2010

Experiment: Tissue Force Characterization

- A corrected position allows us to observe tissue strain
- Controlled constant force application
  - Incremented by 1mN, with 10s delay, over a range of 1-10mN
- Characteristic curve obtained reveals a similar pattern to those seen in fibrous tissue tearing
  - Toe region: Safe
  - Linear region: Predictive
  - Failure region: Peeling

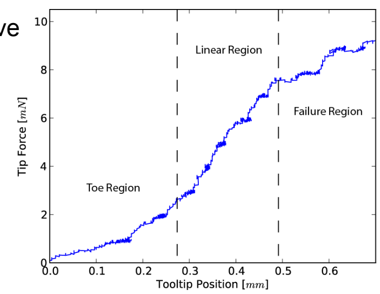

Uneri *et al.*, BioRob 2010

Enhanced Cooperative Control Peeling Algorithm

The algorithm biases operator-robot interaction towards the direction of least tissue resistance while limiting forces.

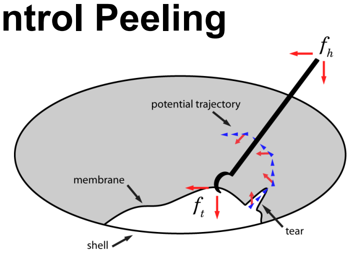

Tape Phantom Peeling

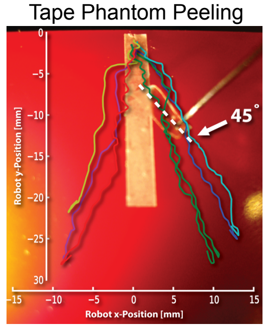

Peeling angles converge to 45 °

Inner Egg Shell Membrane Peeling

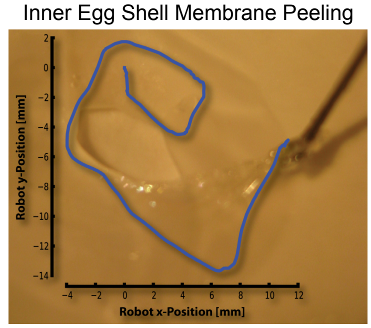

Resulting motion pattern resembles commonly used capsulorhexis technique

Uneri *et al.*, BioRob 2010

Experiment: µForce Guided Cooperative Control

- Task: delaminate PVC strip with acrylic adhesive from a wax surface.
- Strip is peeled at an average of 45°
- User was guided away from the centerline in the direction of lowest resistance

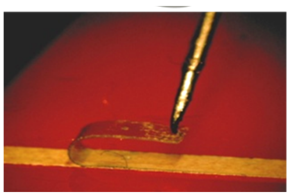

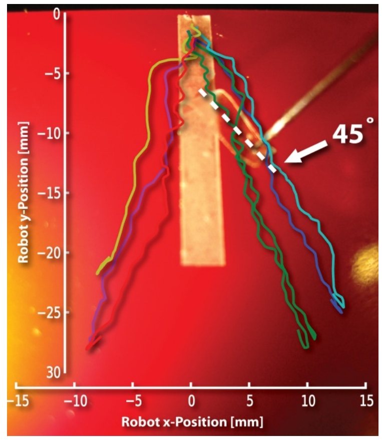

Uneri *et al.*, BioRob 2010

Experiment: µForce Guided Cooperative Control

- Goal: Remove a section of egg inner shell membrane
- Circular trajectory consistent with the results from the strip peeling experiment
- Magnify the perception of tip forces lateral to direction of desired motion
- Results in a peel pattern seen Capsulorhexis maneuver

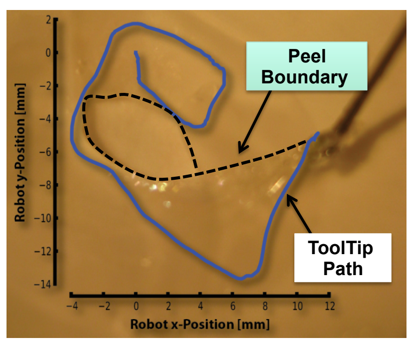

Peeling Inner Egg Shell Membrane

Uneri *et al.*, BioRob 2010

Imaging (OCT) Built Into 0.5mm Surgical Tool

M. Balicki, J. Han, X. Liu, I. Iordachita, P. Gehlbach, J. Handa, R. Taylor, J. Kang.

- Fourier Domain Common Path OCT (FD CPOCT)
- Combined Superluminescent Diodes
- Functional and structural images

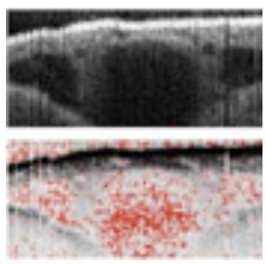

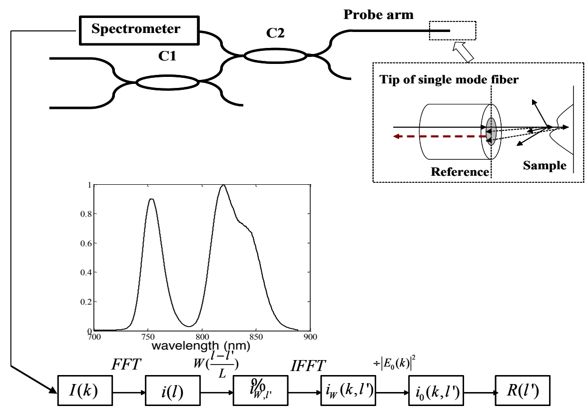

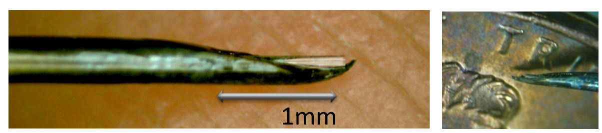

Autonomous Surface Following

M. Balicki, J.-H. Han, I. Iordachita, P. Gehlbach, J. Handa, R. H. Taylor, and J. Kang, *MICCAI 2010*

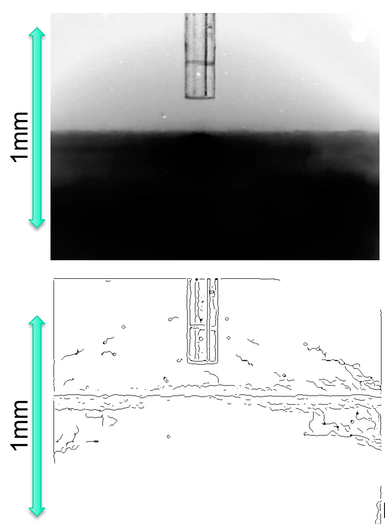

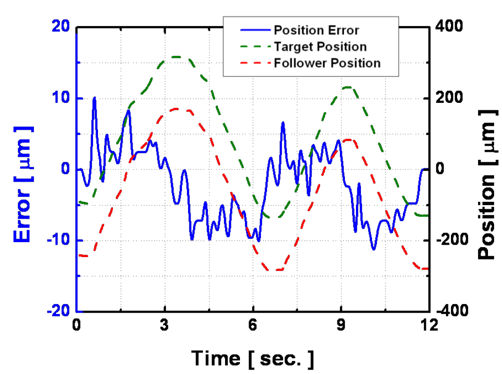

* 500 µm/s Velocity Limit

Noise Rem. /Thresholded/Canny

OCT-feedback in fast hand-held robot

J. Kang, P. Gehlbach, R. Taylor, *et al.*

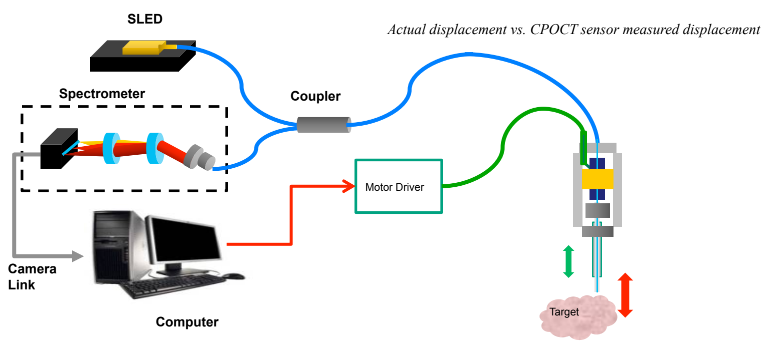

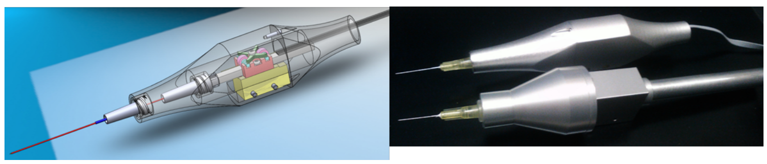

Safety Barrier

J. Kang, P. Gehlbach, R. Taylor, *et al.*

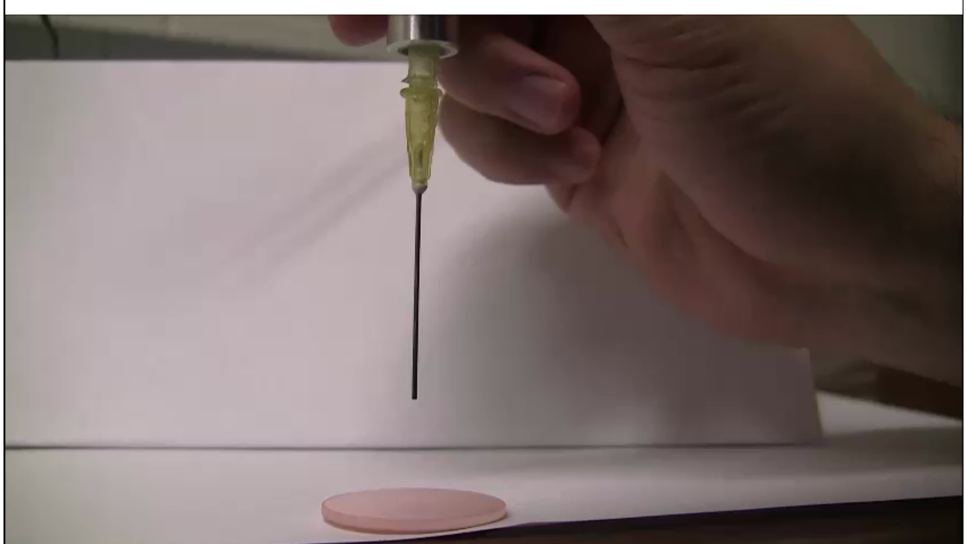

Smart Micro-Forceps

J. Kang, P. Gehlbach, R. Taylor, *et al***.**

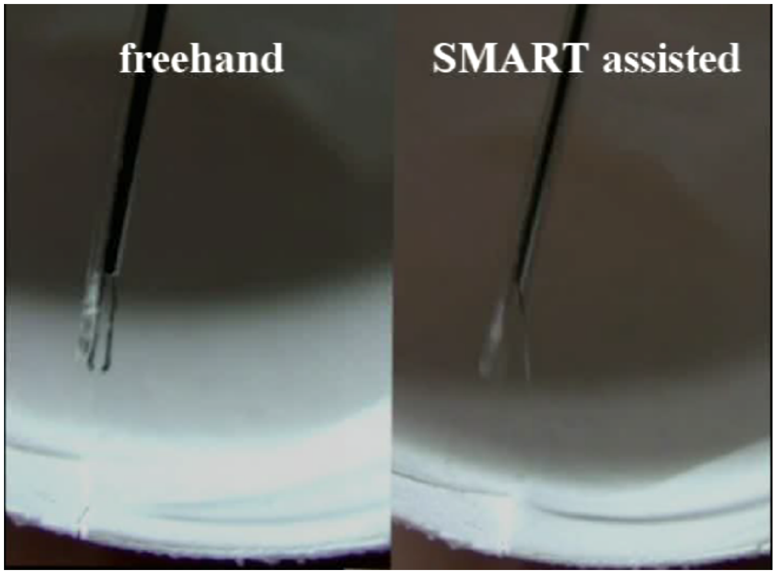

OCT-servoed Injections

J. U. Kang, G.W. Cheon, and P. Gehlbach

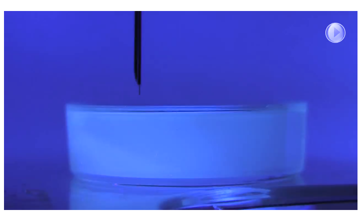

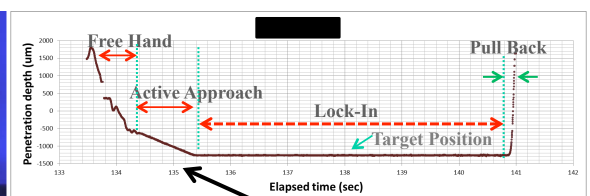

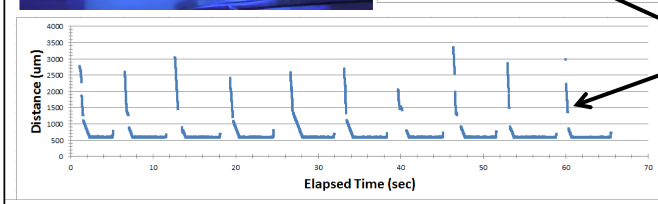

Robot+OCT

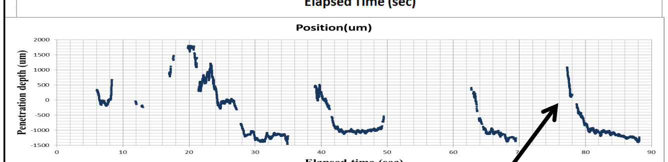

Freehand

Gyeong Woo Cheon, Yong Huang, Hye Rin Kwag, Ki-Young Kim, Russell H. Taylor, Peter Gehlbach, Jin U. Kang, "Injection-depth-locking axial motion guided handheld micro-injector using CP-SSOCT," 36th Annual International IEEE EMBS Conference, 1753, August 2014

GW Cheon, Y Huang, JU Kang, "Active depth-locking handheld micro-injector based on common-path swept source optical coherence tomography," SPIE BiOS, 93170U-93170U-5, 2015.

Robotically-Assisted Insertion of Cochlear Implants

- Setup
  - Phantom cochlea
  - Stiffer stylet
- Surgeon and novice inserted implants into phantom using three methods:
  - Manual insertion
  - Robot-assisted insertion
  - Robot-assisted insertion with virtual fixtures enacted

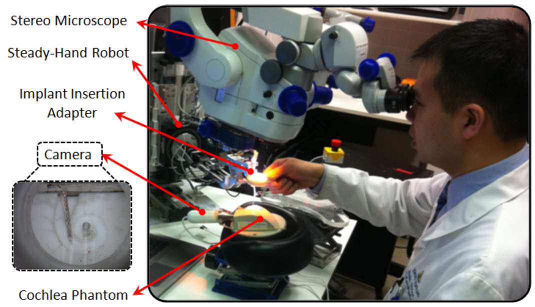

P. Wilkening, W. Chien, B. Gonenc, J. Niparko, J. U. Kang, I. Iordachita, and R. H. Taylor, "Evaluation of Virtual Fixtures for Robot-Assisted Cochlear Implant Insertion", in *IEEE Biomedical Robotics and Biomechanics (BioRob)*, Sao Paulo, 12-15 Aug, 2014. pp. 332-338.

Robotically-Assisted Insertion of Cochlear Implants

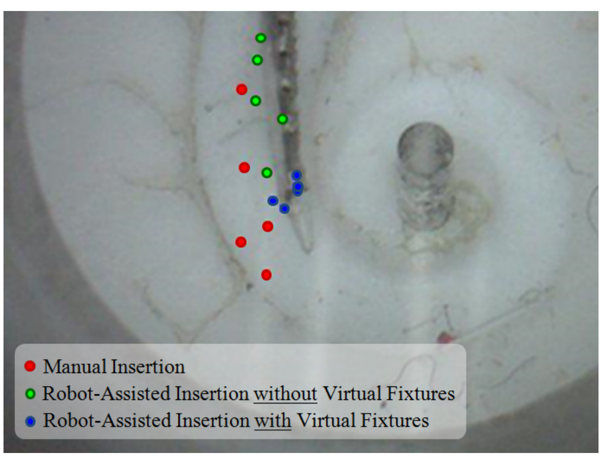

Novice's deployment points

- Each point represents the deployment point reached using one of the insertion methods
- Manual spread very far, not very accurate
- Robot-assisted also spread far, closer to center
- Robot-assisted with virtual fixtures closely clustered and highly accurate

P. Wilkening, W. Chien, B. Gonenc, J. Niparko, J. U. Kang, I. Iordachita, and R. H. Taylor, "Evaluation of Virtual Fixtures for Robot-Assisted Cochlear Implant Insertion", in *IEEE Biomedical Robotics and Biomechanics (BioRob)*, Sao Paulo, 12-15 Aug, 2014. pp. 332-338.

Robotically-Assisted Insertion of Cochlear Implants

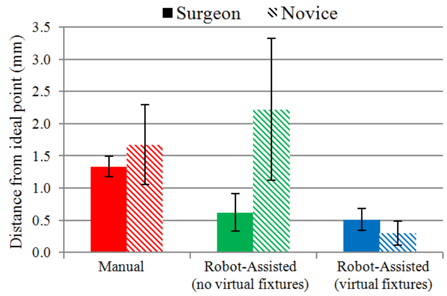

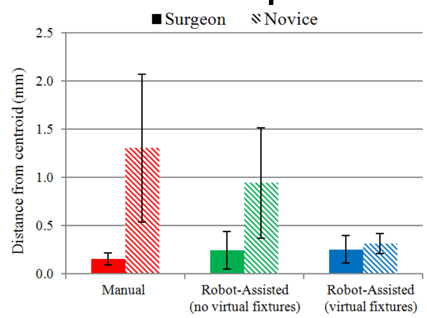

Accuracy Results

- Robot decreases surgeon's mean error by 0.7 mm
- Virtual fixture decreases novice's error by 1.4 mm
- 61.7% mean decrease in accuracy error using virtual fixtures

Repeatability Results

- Robot increased surgeon's repeatability by 0.1 mm
- Novice's repeatability decreased by 0.36 mm, then by 0.63 mm

P. Wilkening, W. Chien, B. Gonenc, J. Niparko, J. U. Kang, I. Iordachita, and R. H. Taylor, "Evaluation of Virtual Fixtures for Robot-Assisted Cochlear Implant Insertion", in *IEEE Biomedical Robotics and Biomechanics (BioRob)*, Sao Paulo, 12-15 Aug, 2014. pp. 332-338.

Information-enhanced robotic surgery

augmented reality displays imaging

safety barriers shared control "virtual fixtures"

SAW

Information-enhanced robotic surgery

augmented reality displays imaging

Tool motions

safety barriers shared control "virtual fixtures"

Information-enhanced robotic surgery

augmented reality displays imaging

Tool motions

Positions

Forces

Fast local compliance law

$\mathbf{F}_c$, other parameters

$\mathbf{F} = [\mathbf{R}, \vec{\mathbf{p}}]$

$\dot{\vec{\mathbf{p}}}$, other state

safety barriers shared control "virtual fixtures"

Virtual Fixture "Hook" in DaVinci API

- **Experimental interface not in any clinical or commercial product.**
- Specification developed jointly by JHU and Intuitive to support research
- Prototyped at JHU by Tian Xia and Russ Taylor
- Current version implemented in DaVinci "S" model by Lawton Verner at ISI, with "hooks" in a proprietary ISI Application Program Interface
- Accessed through cisst/SAW libraries

Compliance virtual fixtures

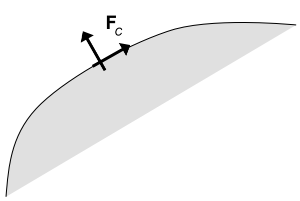

$\mathbf{F} = [\mathbf{R}, \vec{\mathbf{p}}] =$ current pose; $\dot{\mathbf{p}} =$ current velocity

$\mathbf{F}_c = [\mathbf{R}_c, \vec{\mathbf{p}}_c] =$ position compliance frame

$\vec{\mathbf{k}}^{(+)}, \vec{\mathbf{k}}^{(-)} =$ position stiffness factors

$\vec{\mathbf{b}}^{(+)}, \vec{\mathbf{b}}^{(-)} =$ damping factors

$\vec{\mathbf{g}}^{(+)}, \vec{\mathbf{g}}^{(-)} =$ force bias terms

$\mathbf{R}_o =$ orientation compliance frame

$\vec{\mathbf{k}}_o^{(+)}, \vec{\mathbf{k}}_o^{(-)} =$ orientation stiffness factors

$\vec{\tau}^{(+)}, \vec{\tau}^{(-)} =$ torque bias terms

$t =$ time remaining on timeout counter

Compliance virtual fixtures

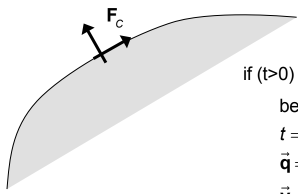

if (t>0) then

begin

$t = t - 1$

$\vec{\mathbf{q}} = \mathbf{F}_c^{-1}\vec{\mathbf{p}} = \mathbf{R}_c^{-1}\left(\vec{\mathbf{p}} - \vec{\mathbf{p}}_c\right)$

$\vec{\mathbf{v}} = \mathbf{R}_c^{-1}\dot{\vec{\mathbf{p}}}$

$\vec{\mathbf{h}} = \vec{\mathbf{0}}; \vec{\psi} = \vec{\mathbf{0}}$

for $i \in \{x,y,z\}$ do

$\left\{\text{if } \vec{\mathbf{q}}_i \le 0 \text{ then } \vec{\mathbf{h}}_i = \vec{\mathbf{g}}_i^{(-)} + \vec{\mathbf{k}}_i^{(-)}\vec{\mathbf{q}}_i + \vec{\mathbf{b}}_i^{(-)}\vec{\mathbf{v}}_i \text{ else } \vec{\mathbf{h}}_i = \vec{\mathbf{g}}_i^{(+)} + \vec{\mathbf{k}}_i^{(+)}\vec{\mathbf{q}}_i + \vec{\mathbf{b}}_i^{(+)}\vec{\mathbf{v}}_i\right\};$

$\vec{\mathbf{f}} = \mathbf{R}_c\vec{\mathbf{h}}$; add $\vec{\mathbf{f}}$ to the forces exerted on the master

$\vec{\theta} =$ Rodrigues vector corresponding to $\Delta\mathbf{R} = \mathbf{R}_o^{-1}\mathbf{R}$

for $i \in \{x,y,z\}$ do

$\left\{\text{if } \vec{\theta}_i \le 0 \text{ then } \vec{\psi}_i = \vec{\tau}_i^{(-)} + \vec{\mathbf{k}}_i^{(-)}\vec{\theta}_i \text{ else } \vec{\psi}_i = \vec{\tau}_i^{(+)} + \vec{\mathbf{k}}_i^{(+)}\vec{\theta}_i\right\};$

add $\mathbf{R}_o\vec{\psi}$ to the torques exerted on the master

end

Surface following virtual fixture

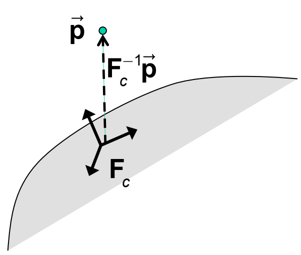

Goal: Stay on a surface; bias force drawing toward the surface; spring force resisting penetration

$$\vec{\mathbf{p}}_c = \text{ closest point on surface}$$
$$\mathbf{R}_c\vec{\mathbf{z}} = \text{ surface normal at } \vec{\mathbf{p}}_c$$

$$\vec{\mathbf{k}}^{(-)} = [0,0,-\textit{stiffness}]$$
$$\vec{\mathbf{g}}^{(+)} = [0,0,-\textit{bias}]$$
$$\textit{Others} = 0$$

Limitation and Extensions

- The specific abstraction just presented has some limitations. In particular, it separates the position and orientation compliance in a way that makes coupling of orientations and translations non-trivial.
- This can be gotten around to some extent by continually updating the virtual fixture compliance parameters.
- There are several obvious extensions that may be tried. For example, one can provide fuller matrices for virtual fixture force/torque generation. For example:

Compute $\vec{\mathbf{q}}, \vec{\mathbf{v}}, \vec{\theta}, \vec{\phi}$ from $\mathbf{F}_c$ and $\mathbf{R}_o$, *where* $(\vec{\phi} = d\vec{\theta} / dt)$

Compute a region *i* of local configuration space from $\vec{\mathbf{q}}$ and $\vec{\theta}$

$$\begin{bmatrix} \vec{\mathbf{h}} \\ \vec{\psi} \end{bmatrix} = \mathbf{K}_i \bullet \begin{bmatrix} \vec{\mathbf{q}} \\ \vec{\theta} \end{bmatrix} + \mathbf{B}_i \bullet \begin{bmatrix} \vec{\mathbf{v}} \\ \vec{\phi} \end{bmatrix} + \begin{bmatrix} \vec{\mathbf{g}}_i \\ \vec{\tau}_i \end{bmatrix}$$

Add $\mathbf{R}_C \vec{\mathbf{h}}$ to master forces and $\mathbf{R}_0 \vec{\psi}$ to master torques